COMPARISON OF ASCE/SEI STANDARD (2010) AND MODAL PUSHOVER BASED GROUND MOTION SCALING PROCEDURES FOR PRE-TENSIONED CONCRETE BRIDGES

A THESIS SUBMITTED TO
THE GRADUATE SCHOOL OF NATURAL AND APPLIED SCIENCES
OF
MIDDLE EAST TECHNICAL UNIVERSITY

BY

MÜGE ÖZGENOĞLU

IN PARTIAL FULFILLMENT OF THE REQUIREMENTS
FOR
THE DEGREE OF MASTER OF SCIENCE
IN
CIVIL ENGINEERING

MAY 2015

Approval of the thesis:

COMPARISON OF ASCE/SEI STANDARD (2010) AND MODAL PUSHOVER BASED GROUND MOTION SCALING PROCEDURES FOR PRE-TENSIONED CONCRETE BRIDGES

submitted by **MÜGE ÖZGENOĞLU** in partial fulfillment of the requirements for the degree of **Master of Science in Civil Engineering Department, Middle East Technical University** by,

Prof. Dr. Gülbin Dural Ünver _____
Dean, Graduate School of **Natural and Applied Sciences**

Prof. Dr. Ahmet Cevdet Yalçıner _____
Head of Department, **Civil Engineering**

Assoc. Prof. Dr. Yalın Arıcı _____
Supervisor, **Civil Engineering Dept., METU**

Examining Committee Members:

Assoc. Prof. Dr. Alp Caner _____
Civil Engineering Dept., METU

Assoc. Prof. Dr. Yalın Arıcı _____
Civil Engineering Dept., METU

Assoc. Prof. Dr. Afşin Sarıtaş _____
Civil Engineering Dept., METU

Assoc. Prof. Dr. Ayşegül Askan Gündoğan _____
Civil Engineering Dept., METU

Gizem Seyhun, M.Sc. _____
ZTM Engineering and Consulting Co.Inc.

DATE: 04.05.2015

I hereby declare that all information in this document has been obtained and presented in accordance with academic rules and ethical conduct. I also declare that, as required by these rules and conduct, I have fully cited and referenced all material and results that are not original to this work.

Name, Last Name: Müge Özgenoğlu

Signature :

ABSTRACT

COMPARISON OF ASCE/SEI STANDARD (2010) AND MODAL PUSHOVER BASED GROUND MOTION SCALING PROCEDURES FOR PRE-TENSIONED CONCRETE BRIDGES

Özgenoğlu, Müge
M.S., Department of Civil Engineering
Supervisor: Assoc. Prof. Dr. Yalın Arıcı

May 2015, 89 pages

The seismic design and evaluation of large bridges is a demanding task owing to the significant size and the structural characteristics of these systems. Although elastic analysis methods are regarded as sufficient for common, uncritical bridges; complex analysis methods such as non-linear time history analysis (NTHA) are often required for non-standard and/or important bridges. The selection of the ground motions that will be used in non-linear time history analysis is a crucial task in this regard as the results of time history analyses will show a wide variability according to the utilized earthquake record. Furthermore, in order to predict the expected demand in accordance with the seismic hazard conditions of the site, the selected ground motions are usually modified by the scaling procedures. A separate but equally important goal is to obtain the engineering demand efficiently with a small number of representative motions. Within this context, in this study, the relative performance of two ground motion scaling methods, namely the Modal Pushover Based Scaling (MPS) and ASCE/SEI Standard (2010) procedures, are investigated using a number of ground motion sets selected from a suite of 35 ground motions for the NTHA of a representative large

bridge, the Demirtas Viaduct. The system, composed of 28 spans and various expansion joints, is idealized with two different analytical models. Three different target earthquake levels are used for both models in order to determine the effect of the scaling of the ground motions at different hazard levels. The final goal of the study is to establish the sensitivity of the demand parameters and the efficiency of the ground motion scaling techniques considering different target demand levels and structural models.

Keywords: Seismic analysis of bridges, Non-linear time history analysis, Ground motion scaling, ASCE/SEI, MPS method

ÖZ

ASCE/SEI (2010) VE MODAL İTME ANALİZİ TEMELLİ ÖLÇEKLENDİRME YÖNTEMLERİNİN ÖN-ÇEKİM KÖPRÜLERDE KARŞILAŞTIRILMASI

Özgenoğlu, Müge
Yüksek Lisans, İnşaat Mühendisliği Bölümü
Tez Yöneticisi: Doç. Dr. Yalın Arıcı

Mayıs 2015, 89 sayfa

Büyük köprülerin sismik tasarımı ve değerlendirilmesi, işlevsel ve yapısal özelliklerinden dolayı özel çaba gerektiren bir iştir. Kritik olmayan, sıradan köprüler için elastik analiz yöntemleri yeterli görülmesine rağmen; standart olmayan, önemli köprüler için elastik ötesi zaman tanımlı analiz gibi karmaşık analiz yöntemlerinin kullanılması gerekebilmektedir. Elastik ötesi zaman tanımlı analiz yöntemi uygulanırken kullanılan deprem kaydına göre analiz sonuçları önemli ölçüde değişkenlik göstereceğinden deprem kayıtlarının belirlenmesi çok önem kazanmaktadır. Bunun yanında sahadaki sismik tehlike şartlarının oluşturacağı beklenen istemlerin modellerde doğru öngörülmesi için seçilen yer hareketleri genelde ölçeklendirilmektedir. Analizler için diğer bir önemli amaç ise yapısal istemleri az sayıda temsili deprem hareketi kullanılarak etkin bir şekilde elde etmektir. Bu bağlamda, bu çalışmada iki ölçeklendirme metodunun, yani Modal İtme Analizi Temelli Ölçeklendirme (MPS) ve ASCE/SEI (2010) Ölçeklendirme yöntemlerinin karşılaştırmalı performansı, 35 deprem hareketinden elde edilen çeşitli deprem hareketleri grupları ile seçilen köprü örneği Demirtaş Viyadüğü üzerinde elastik ötesi analizler ile incelenmiştir. Seçilen sistem, 28 açıklık ve birkaç genleşme derzinden oluşmakta olup, iki değişik analitik model ile idealize edilmiştir.

Ölçeklendirme prosedürlerinin değişik sismik tehlike seviyelerindeki etkilerini incelemek için bu modeller üç değişik tehlike seviyesinde analiz edilmiştir. Bu çalışmanın ana amacı değişik yapısal modeller ve çeşitli tehlike seviyeleri için istem parametrelerinin hassasiyetinin ve ölçeklendirme yöntemlerinin efektifliğinin belirlenmesidir.

Anahtar Kelimeler: Köprülerin sismik analizi, Elastik ötesi zaman tanımlı analiz, Yer hareketi ölçeklendirme, ASCE/SEI, MPS yöntemi

To my family

ACKNOWLEDGEMENTS

This study was conducted under the supervision of Assoc. Prof. Dr. Yalın Arıcı. I would like to express my sincere appreciations for his guidance, invaluable support, recommendations and insight throughout the research. His careful evaluation and endless patience provided to finish this dissertation.

I am also grateful to the members of my thesis examining committee; Assoc. Prof. Dr. Alp Caner, Assoc. Prof. Dr. Ayşegül Askan Gündoğan, Assoc. Prof. Dr. Afşin Sarıtaş and Gizem Seyhun for their willingness to help, productive comments and contributions to this study. I sincerely thank to Erhan Karaesmen and Engin Karaesmen for their kind and friendly advices, and their always smiling faces to me.

My beyond lovely thesis-sisters, Gizem Mestav Sarıca and Arzu İpek Yılmaz made everything easier for me in this process. I am deeply thankful for their motivation, encouragement, continued support and advices on solving any type of problems that I had encountered in this process. The time that I have passed with them was always enjoyable and worthwhile for me. I am also thankful to my friend Serhad Sarıca for his crucial helps while challenging with "word" and Ali Bulut Üçüncü for his smart advices at critical times.

I would also like to thank to the instructors and research assistants in Structural Mechanics Department of METU Civil Engineering Department for their contributions to my knowledge throughout my study. I would like to express my special thanks to Mustafa Can Yücel, Ahmet Kuşyılmaz, Alper Özge Gür and Kaan Kaatsız for their kind friendship besides of their helps anytime that I need. Getting together with them always made me happy and inspired. I would also like to acknowledge my colleague Mustafa Berk Duygu for his help and advices throughout this study. My another special thanks is for my precious friends Sinem Çelebiöven, Cevahir Karagöz, Hande Boranbay and Pınar Tunca for their amusing and unforgettable contributions to my life and standing by me all the time.

I also thank to the instructors in Technology Faculty Civil Engineering Department of Gazi University and research assistants Pınar Sezin Öztürk, Rüya Kılıç Demircan, Murat Pınarlık, Kenan Toklu Anıl Özdemir, Mustafa Dayı and Baran Toprak for their friendship and continued support. I am very pleasant to be working with them.

My deepest thanks is for my sweet and wide family. Their continuous love, understanding and motivation. always made me in secure and stronger. I express my deepest love and special thanks to each member of my family who is with me and lives in my heart.

TABLE OF CONTENTS

LIST OF TABLES

TABLES

LIST OF FIGURES

FIGURES

CHAPTER 1

INTRODUCTION

1.1 GENERAL

Concrete highway bridges are usually considered to be simple structural systems since they are comprised of a limited number of elements. However, they are actually complicated structural systems, as they consist of interconnection of different types of elements which also differ according to the bridge type. Although the simplicity of bridges provides for a more realistic prediction of the seismic response; it also increases the sensitivity to the design errors. In addition, having little or no redundancy makes bridges more likely to collapse when they lose a structural element or connection. Another challenge about bridge structural characteristics is that bridges, especially long-spanned bridges, are more susceptible to soil-structure interaction effects because each bridge support may be exposed to different seismic input. Moreover, as it is not possible to change the location of bridges most of the time, difficulties resulting from the ground conditions like crossing rivers or active faults can be confronted frequently. All of these considerations, along with the critical nature of bridges in transportation infrastructure, indicate that special care should be taken for seismic design of bridges (Priestly et al. 1996). Besides these concerns related to the characteristics of bridges, in the past earthquakes like Loma Prieta (1989), Northridge (1994) and Kobe (1995) Earthquakes, bridges have shown unexpectedly exhibited poor behavior demonstrating that the conventional methods for the seismic design and evaluation do not provide adequate performance (Priestly et al. 1996, Kawashima 2000). Therefore, studies regarding the seismic design, evaluation and the construction of bridges have gained speed since these destructive events.

For the seismic analysis of bridges both elastic and inelastic methods exist in the design codes. Although elastic methods can be sufficient for the design of standard bridges, inelastic dynamic analysis, in other words non-linear time history analysis, is considered necessary for some cases. In the use of non-linear time history analysis (NLTHA), besides many uncertainties, the selection of ground motions is one of the most important concerns because the response of the structure shows a wide variability according to the input earthquake record. During the selection of the ground motion records, several criteria should be considered. However, the implementation of a special selection procedure is not sufficient to predict the "true" demand for the structure. The demand on the structure is traditionally represented by response spectrum in earthquake engineering, therefore, the selected ground motions are generally subjected to a scaling procedure in order to conform to the target demand levels defined by the response spectrum. The "true" response of a structure can be considered as the mean response of a large number of earthquake motions likely to happen at the site. The ground motions should be selected and scaled such that the structural demands attained from the analysis with those records should be close to the "true" demand for the structure.

In literature and design codes various scaling methodologies are provided, but the validity of these methods for different structures is still a research topic.

1.2 LITERATURE RESEARCH

The variation in the response parameters in time history analysis has revealed the necessity of specifying a selection criterion for earthquake motions that will be used in the analysis and scaling the selected motions. However, for this issue, little guidance is present in design codes leading the engineers to make choices according to their personal perspective which raises the uncertainty of the analysis results (Donnell et al., 2013).

The aim of the selection and scaling of the records is to obtain accurate, consistent and efficient results from the time history analysis. "Accuracy" represents the ability to predict the true response of the structure under the predetermined seismic level and site conditions with a small group of selected and scaled earthquake records. "Consistency" is used to examine the invariability of the results between the different

sets of records, i.e. the difference between two engineers working on the same structure and seismic demand target with different sets of motions should be ideally minimal. Finally, "efficiency" is associated with the discrepancy between records in the set (Reyes et al., 2012). A high discrepancy within the results of a ground motion set would imply the possibility of different behavior of the structure for the same target level which would require more time and effort to scrutinize and evaluate the analysis results. Considerations for selecting the records and scaling procedures are summarized in the following sections.

1.2.1 Ground Motion Selection for Time History Analyses

Time histories that will be used in seismic design and evaluation should be appropriate to the design earthquake. They can be obtained by selecting and scaling real earthquake records, generating artificial records fitting to the design response spectrum and producing synthetic records according to an earthquake source (Bommer et al., 2000a). In order to implement the first and third procedure, determination of an earthquake scenario is required. For the second approach, only design spectrum is necessary (Bommer et al., 2000a).

Determination of a selection criterion according to seismic hazard conditions of the site decreases the dispersion in demand parameters received from non-linear time history analysis. The main parameters that mostly affect the spectral shape of an earthquake record are the magnitude of the event, distance to the active fault, site conditions, basin effect and directivity. Earthquakes with greater magnitudes yield response spectra in wider forms and predominant period moves to higher periods (Graizer et al., 2010). Increase of the distance to the fault also causes the predominant period of response spectrum to shift to higher periods. Site conditions affect the frequency content as well: the predominant period of the spectrum takes smaller values in rock sites (Abrahamson et al., 1997) or higher values over soft soil deposits. Duration of ground motions is regarded as a secondary parameter on structural damage since duration of an earthquake depends on mostly the magnitude of the event which has already been considered (Bommer et al, 2000b; Hancock et al., 2007). For the selection of earthquake records, general approach is to consider the magnitude of the event, distance to the fault and soil conditions. However, it

should not be forgotten that directivity and the basin effects also influence the frequency content and intensity of the shaking at the site (Donnell et al. 2011).

In design specifications, it is indicated that the selected ground motions should be in accord with the design spectrum of the site. ASCE /SEI 07 recommends the consideration of the magnitude, source mechanism and the fault distance features of the earthquake events. In terms of the number of records, the use of at least three records is recommended if the maximum of the engineering demand parameter among the three motions is used. It is permitted to use the mean value of EDPs if seven or more than seven motions are chosen for time history analysis in ASCE/SEI 07 as well as other design specifications. If the number of suitable records is not enough, simulated motions can be utilized to complete the suite to the required number.

The suggestions in ASCE/SEI 07 appear to be determined according to the engineering experience (Reyes et. al, 2012). Reyes and Kalkan (2012) studied a range of single degree of freedom nonlinear systems with elastic-perfectly plastic and bilinear response in order to investigate validity of these recommendations. According to their work, using less than seven records does not provide efficient and consistent results and accurate values are obtained when seven or more motions are utilized. However, increasing the number of records from 7 to10 in time history analysis does not affect the accuracy considerably.

EUROCODE 8 (EC8) also proposes that at least three ground motion records should be selected for non-linear time history analysis considering the magnitude, distance to the source and mechanism suitable to the design seismic event. If earthquake records representing the design seismic event are not present, the modified or simulated records can be used. If more than seven records are selected, then, the mean values of the demand parameters can be used instead of maximum values. The horizontal components of the accelerograms are combined with the “Square Root of the Sum of the Squares” (SRSS) rule and the average spectrum of the three records is scaled such that it will be 1.3 times greater than the design spectrum for the range from $0.2T_1$ to $1.5T_1$, where T_1 is the fundamental period of the bridge. Then the scale factor is applied to the selected ground records. If the ratio of acceleration values of SRSS spectra of the records to those of design spectrum exhibits a large variability,

then the records may be subjected to modification process to be close to the design spectra. EC8 also specifies the application of vertical component of the earthquake records.

AASHTO (2012) suggests selecting ground motions considering tectonic conditions, earthquake magnitude, faulting type, distance to the fault, site conditions and design or expected ground motion characteristics. However, magnitude and distance parameters are considered as the most important criteria since they affect spectral shape and content, duration of ground shaking and near fault motion characteristics. For scaling and/or modification of selected motions, AASHTO (2012) recommends scaling the selected ground motions to approximate the design spectrum before applying spectral matching.

1.2.2 Scaling of Ground Motions for Time History Analyses

Ground motion scaling procedures can be grouped as spectral matching methods (Lilhanand et al., 1988) and amplitude scaling methods (Katsanos et. al 2010).While amplitude scaling methods just change the intensity of the record, spectral matching procedures modify both the amplitude of the record and the frequency content to catch the target spectrum (Kalkan et al., 2010).

Initial applications of response spectrum matching techniques uses artificial records produced from white noise rather than the real records (Reyes et al. 2014). However, for the structures displaying non-linear behavior, this technique is found inefficient and inaccurate since artificially obtained records may have unrealistic characteristics (Hancock et al. 2006). In using actual accelerograms, modification in frequency domain creates distortion in velocity and displacement time series causing time history records having insensible energy content whereas altering the records in time domain by inserting wavelets keeps the actual non-stationary aspects of the records (Naeim et al., 1995; Hancock et al., 2006).

In the study of Reyes et al., (2014) the scaling method in ASCE/SEI 7-16 is mentioned. The draft version of ASCE/SEI 7-16 permits the modification of ground motions with spectrum matching techniques After spectrum matching, each component of the time histories is scaled such that the mean spectrum of records will

be greater than the target spectrum for the range between $0.2T_1$ and $2.0T_1$ which is more rigorous method compared to amplitude scaling However this method is limited for use on only far field records, because after spectrum matching pulse characteristics may not be kept in proper manner (Reyes et al. 2014). Ground motions modified by spectrum matching can cause underestimations for non-linear seismic analysis according to some researchers while this opinion is not shared by others (Reyes et al. 2014).

In the study of Heo et al. (2011) spectrum matching and scaling records to target spectral acceleration at fundamental period are examined on reinforced concrete moment frame buildings. According to this study, spectrum matched records give more accurate and efficient results compared to the used amplitude scaling method. Another finding of this study is the increase in the variability of the results with the increase in the complexity of the structure.

In amplitude scaling methods, scale factors are procured for a small number of earthquake records. The objective is to obtain response values close to the "true" median response of the structure and to decrease the variation in response results with small number of scaled records (Kalkan et al. 2010). Early amplitude scaling methods were based on the intensity measure parameters which are peak ground acceleration (PGA), Arias Intensity, effective peak acceleration and effective peak velocity. However, these procedures generally yield inaccurate results with large variation for inelastic structures (Kurama et. al, 2003; Shome et al., 1998). Scaling methods which take the structural properties into the consideration like fundamental period of the structure and structural capacity have later been developed. Scaling records to a spectral acceleration at the first mode of the structure provided improved insight to the scaling process (Shome et al. 1998). However, for the structures exhibiting higher mode response or responding in the inelastic range, scaling to the first mode spectral acceleration leads to less accurate and less efficient results (Kurama et al., 2003). For higher mode consideration an Intensity Measure (IM) scalar and a vector were defined which depends on the spectral acceleration at first and second mode spectral acceleration (Bazzurro, 1998; Shome et al. 1999). This advance increased the accuracy but was not found effective for near fault time histories having dominant velocity pulse (Baker et. al 2006). Since the period of the

structures increases after yielding, another IM scalar depending on the spectral acceleration at first mode period A (T_1) and at a period which is greater than the first mode period A(cT_1) is determined (Mehanny, 1999 ; Cordova et al., 2000). However, these scalars do not regard the inelastic behavior of the structure directly and only depend on the elastic vibration period of the structure (Kalkan et al., 2010). In case of near fault excitations, in which the inelastic deformations may occur in considerable level, the scaling procedures depending on the inelastic deformation spectrum or the deformation of the first mode inelastic single degree of freedom systems (SDOF) were found more sufficient (Luco et. al 2007, Tothong et al., 2008) Modal pushover based scaling (MPS) method which was developed by Kalkan and Chopra uses these approaches (Kalkan, et. al, 2012).

The accuracy and efficiency of MPS procedure has been demonstrated for different types of structures. In the study of Kalkan and Chopra (2010), low-, mid- and high-rise building structures are analyzed with the motions scaled by MPS and ASCE/SEI 7-05 procedures. According to this research, MPS method gives more accurate results compared to ASCE/SEI 7-05 procedure. MPS procedure is also tested for "Ordinary Standard Bridges"; Kalkan et.al. (2012) verified that MPS yields demand parameters close enough to the considered benchmark with low dispersion for one component analysis of single bent over-pass bridge and multi-span bridges. According to this study, it is observed that the accuracy decreases in case of two component analysis of irregular bridges compared to the former case.

MPS, ASCE and two other scaling methods, namely scaling to the maximum incremental velocity (MIV) and non-stationary spectral matching (RSPM) were investigated for concrete gravity dams in the study of Duygu (2014).While, MPS and MIV procedures yield more accurate results, ASCE and RSPM scaling were observed to yield demand values with lower dispersion.

Applicability of scaling methods is tested on building type of structures much more than the other structural systems. Donnell et al. (2013) investigated four scaling methods which are ASCE 7-10 scaling procedure, scaling to the geometric mean of maximum incremental velocity (MIV), scaling records to the geometric mean of spectral acceleration at fundamental period of the structure, and finally modal pushover based scaling (MPS) for multi-story building frame structures having

different fundamental periods. In this study, the results obtained by MIV scaling procedure possess the least dispersion while MPS scaling was observed to yield mean values at the conservative side. Among these four methods, MIV is independent of the structural characteristics like fundamental period and the capacity of the structure. Therefore, MIV eliminates the mistakes related to the modeling of the structure (Donnell et al. 2013).

Ground motion scale factors are generally preferred close to unity: many researchers argue that there should be limiting values for the scale factors with maximum limits ranging from 2 to 4 (Bommer et al., 2004). In the study of Watson-Lamprey and Abrahamson (2005), conventional record selection; which is based only on the magnitude, distance and site condition; and an improved method for selection were investigated to approximate the average value of a large suit of ground motion. According to this study, if selection is carried out based on the magnitude, distance and site condition parameters, the limits for scale factors were found appropriate.

1.3 SCOPE AND OBJECTIVE

The primary objective of this study is to compare ASCE/SEI Standard (2010) scaling and the modal pushover based scaling (MPS) methods for complex bridge models at different seismic demand levels. In this scope;

- Two models of the Demirtas Viaduct are prepared and selected as case studies differing from each other in terms of number of spans. Elastic material properties are used to obtain natural frequencies and mode shapes of the bridge models.
- Considering the properties of the site on which the Demirtas Viaduct is located, 35 different ground motions are selected from the PEER Strong Motion Database (PEER, 2013). These 35 earthquake records are scaled according to ASCE/SEI (2010) scaling procedure and the Modal Pushover Based Scaling (MPS) procedure.
- Scaling is conducted for three different seismic levels in order to determine the effect of the target level on the results. Three target spectra are used: the first target is selected as the mean of the 5% damped response spectrum of unscaled motions corresponding roughly to a 144-year event. AASHTO

(2010) design spectrum for 1000-year earthquake event and (DLH) design spectrum for 2475-year earthquake event are used as the higher target levels. Since only the mean spectrum of a large set of motions was utilized for the evaluation of scaling procedures in previous studies, design spectra are also employed to test the validity of these methods as a novel part of this study. Given a suitable mean spectra determined for a large group of earthquake records is very difficult to obtain for a site with seismic hazard conditions, a mean spectrum is not always convenient for practical use in a design process.

- The scaled accelerograms are randomly separated into 5 sets and the non-linear time history analysis with scaled ground motions is carried out for each set in the transverse direction (perpendicular to the roadway). With three target spectra and two bridge models, 32 analysis cases are obtained for each scaling method. ((5 sets)x(3 earthquake levels)x(2 bridge models) + (2 extra sets for third earthquake level))
- The results are then compared to each other for different scaling methodologies (ASCE/SEI07, MPS), target spectrum levels (144, 1000, 2475 year return period events) and the modeling approach. Accuracy, consistency and efficiency are evaluated in this context.

The novel contributions of this study for the seismic analyses of the bridges are:

- ASCE/SEI 07 and MPS methods are compared for the first time for the case of a complex bridge system. These methods were evaluated only for building systems and single bent simple overpasses in the past.
- The scaling procedures have been evaluated for a single seismic demand level, as defined by a target spectrum, in the past studies. Three different levels of seismic demands are considered here for the first time in order to assess the level of seismic demand on the time history scaling approach.
- The complex behavior of a large system could be modeled using different models with an accuracy/cost tradeoff. The effect of the modeling approach to the ground motion scaling is also evaluated for the first time for a complex bridge system in this study.

The limitations of this study are presented as follows:

- The effect of possible multiple-support excitation on the bridge model is not considered given obtaining such motions would constitute a separate scientific study outside the scope of this work.
- The nonlinearity on the system is assumed to be only due to the behavior of column-bents. The superstructure of the system as well as the bearings is assumed to behave linear elastic.
- The pile-foundations under the column-bents are not included in the analysis and the bases of the columns are assumed as fixed supports.

The goal of the study is the evaluation of the scaling methodologies for time history analyses of motions for the case of complex bridge systems. These simplifying assumptions are made in order to simplify the scope and reach clear conclusions on the use of scaling methodologies for seismic design. The assessment of the structural behavior of the Demirtas Viaduct is not attempted in this study.

This thesis is composed of 5 Chapters. Information on the seismic design/analysis methodologies for bridge systems are presented in Chapter 2, along with the definition of the case study, the Demirtas Viaduct. The selection of ground motion records, the target spectra and the scaling methods are explained in Chapter 3. The results of the nonlinear time history analyses are presented and evaluated in Chapter 4. The conclusions of the study are presented in Chapter 5.

CHAPTER 2

SEISMIC ANALYSES METHODOLOGY FOR BRIDGES AND THE CASE STUDY, THE DEMIRTAS VIADUCT

2.1 INTRODUCTION

Seismic analysis methods of bridges can be examined under the headings of elastic and inelastic analysis methods. Applicability and restrictions on the use of seismic analysis methods for bridges are usually given in the respective design manuals and specifications given the tradeoff between the time and accuracy regarding the use of any given method for seismic design or evaluation. The selection of the analysis method depends on a set of criteria like the span lengths, number of spans, the importance of the bridge, soil conditions of the site and the objective of the analysis. The general approach in design manuals is the use of elastic methods for the determination of engineering demand parameters (EDP), such as top displacements or base shear demands, which are often used as critical parameters in a design/evaluation process.

According to CALTRANS Specifications (2013), for "Ordinary Standard Bridges" (OSB), Equivalent Static Analysis and Response Spectrum analysis can be used for the estimation of displacement demands and Inelastic Pushover Analysis method can be used for the estimation of the displacement capacities. The following properties are given as the traits of "Ordinary Standard Bridges" for which these methods may be used for seismic design:

- Span length is smaller than 90 m,
- Normal-weight concrete is used,
- Foundations are on spread footings,

- The soil should not be sensitive to liquefaction or lateral spreading during ground shaking (CALTRANS 2006)

Elastic analysis methods are sufficient for OSB built in regions with low-seismicity. However, when bridges are subjected to high seismic hazard and near fault effects are present, the expected structural response moves from the elastic to inelastic range (Goel et al., 2008; Kalkan et al., 2006). Therefore, non-linear time history analysis; which requires ground motion selection and modification, is necessary for the prediction of the nonlinear behavior of these bridges in case of near-fault events (Kalkan et al., 2012). According to AASHTO LRFD Seismic Bridge Design (2011) Specification, nonlinear time history analysis is suggested for class-D seismic design category (SDC-D) or in case seismic isolation is considered in design. SDC-D is applied if design spectral acceleration at 1 second is greater than 0.5 (g) or lateral-spreading or slope failure hazard is present in the site.

2.1.1 Modeling and Elastic Analyses

PEER guidelines for nonlinear modeling and CALTRANS specifications are utilized to constitute the computer models. For modeling, the following aspects are recommended:

- Three-dimensional modeling with line elements is the customary approach for constructing analytical bridge models. Superstructure, cap beam and columns are modeled with line elements passing through their geometrical centroids. The bridge components are divided into different number of elements according to their lengths. It is suggested that superstructure, cap beams and columns should consist of minimum 5 elements having equal length to provide accurate mass distribution.
- For material definition, effective material properties should be used in order to predict the exact capacity and the behavior of the bridge. CALTRANS SDC requires the use of concrete properties according to their own criteria and the confined and unconfined models by Mander et. al. (1988) for constitutive behavior of concrete. The consideration of concrete tensile strength is also recommended.

- Translational mass is assigned to the nodes as lumped masses in longitudinal, transverse and vertical directions considering the tributary lengths. Translational masses can be defined automatically by the software or defined by the user according to employed computer program. In addition to the translational masses, rotational masses are assigned when a global torsional mode is induced.
- Linear-elastic beam-column elements with cracked reinforced concrete properties should be used to model superstructure elements.
- Superstructure cross-sectional properties should be computed accurately utilizing a separate spreadsheet or a program. A rectangular cross section having the total height and width of the superstructure should not be used, because it causes overestimation in stiffness and mass of the superstructure.
- For reinforced concrete superstructure components, as cracking of the concrete occurs before the yielding of the section, moment of inertia of the superstructure should be exposed to a reduction factor, i.e. effective moment of inertia should be used. It is important in order to get more realistic fundamental periods of the structure and structural demands. The use of effective torsional moment of inertia is not required for superstructures of OSB.
- Pre-stressing forces are defined if the superstructure displays inelastic behavior. However, for the bridges meeting OSB features, superstructure is modeled with cracked elastic properties.
- For columns, inelastic beam-column elements with cracked flexural stiffness are utilized. Since torsional stiffness decreases considerably after cracking, effective torsional resistance J_{eff} should be defined as 0.2 times of torsional inertia of gross section.

For multi-frame analysis, CALTRANS (2013) suggests the modeling of bridges with at least two boundary frames or one frame and one abutment. The modeling criteria can be seen from the Figure 2-1. Long multi-framed bridges are modeled with several sub-models since a single model cannot explain out of phase movement of the frames. The sub-models should overlap with minimum one frame from out of the

boundary frame or abutment. Since the boundary frame does not correspond to the complete structure behavior, the results obtained from the sub-models have to be evaluated and interpreted by the engineer.

Massless springs representing the stiffness of the rest of the structure are suggested for the ends of the boundary frames. However, any information related to the definition of the properties of these springs at the end of the boundary frames is not provided in the design manuals.

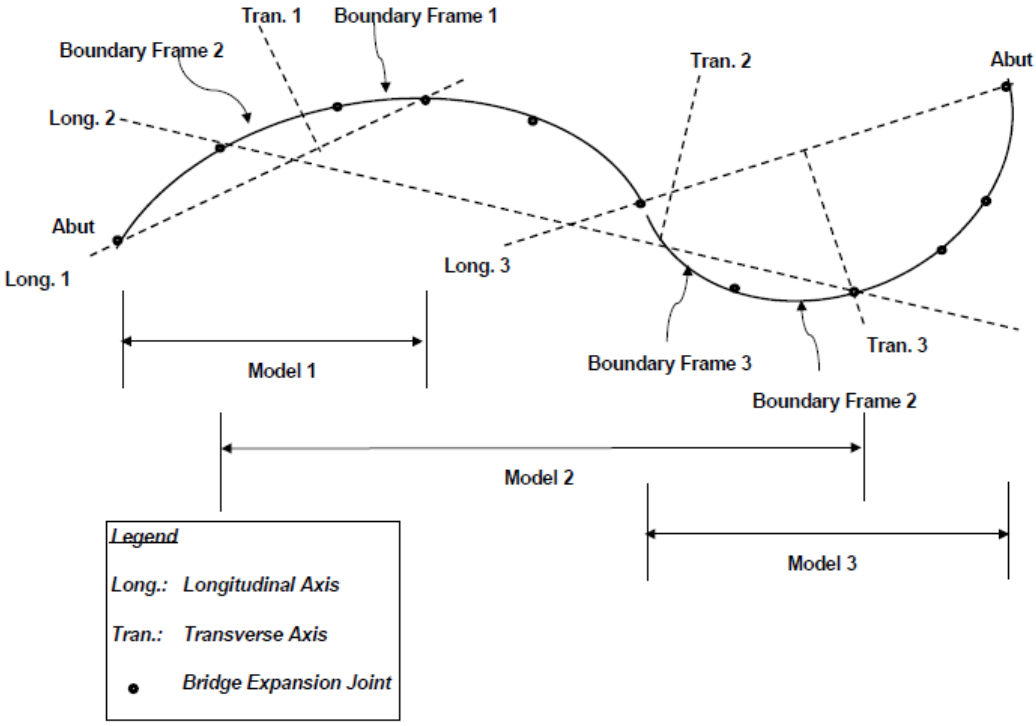

Figure 2-1 Modeling Techniques for Elastic Dynamic Analysis (adopted from CALTRANS SDC-1.7)

Modal analysis is used to obtain the dynamic properties of a structure which are required for assessing the spectral demand on the structure. The main parameters in terms of structural dynamic characteristics, the natural periods and modal shapes of the structure, are used as defining parameters within the ground motion scaling procedures. These parameters are estimated depending on the mass and stiffness of the structure. In OSB, the primary modes arise as longitudinal and lateral translation, global torsion and flexural contortion of the superstructure (Aviram et. al 2008).

2.1.2 Non-Linear Analyses

The nonlinear characteristics of the structure may be seen in two different ways. The first reason of non-linearity is the inelastic behavior of elements and the sections due to non-linear material properties and the existence of the dampers, gaps or non-linear spring components. The second reason of non-linearity includes the second-order effects or P-Δ effects which are considered as the geometric non-linearity. (Aviram et al., 2008).

In non-linear modeling of bridges, general approach is to model superstructure elements elastically; inelastic modeling is deemed necessary only for abutments, expansion joints and column plastic hinge zones (Table 2-1). Modeling of nonlinear pile foundation is an area of extensive study.

Table 2-1 Suggested Bridge Modeling (adopted from Aviram et al., 2008)

Component	Linear Elastic	Nonlinear
Superstructure	x	
Column-plastic hinge zone		x
Column-outside plastic hinge zone	x	
Cap beam	x	
Abutment-transverse		x
Abutment-longitudinal		x
Abutment-overturning		x
Abutment-gap		x
Expansion joints		x
Foundation springs	x	
Soil Structure interaction	x	

True estimation of inelastic properties of the bridge elements is also important to provide the reliability and accuracy of the results.

2.2 CASE STUDY – THE DEMIRTAS VIADUCT

Demirtas Viaduct, a very long highway bridge located in Bursa beltway, is chosen as the case study for this thesis. The bridge is an important connection on the prominent transportation route on the motorway between İstanbul and İzmir located in the first degree seismic zone. The Demirtas Viaduct is actually composed of two parallel systems, separated by a 1.5 m gap between the roadways. Both of the bridges have 28 spans, a 2.85% slope in the longitudinal direction and are almost identical excluding the pier heights due to the local topography. For the purposes of this study, one of the roadways is chosen and modeled. The span length of the selected bridge is 39 m at the middle spans and 37 m at the first and last spans. The total length of the bridge is 1088 m. The elevation view of a segment of the bridge is shown in Figure 2-2 and the whole bridge is provided in Appendix C.

According to a previous study (Sevgili, 2007), the span length of the Demirtas Viaduct is not very common for the bridges in Turkey. However Demirtas is representative of a considerable portion of bridges in Turkey given the typical superstructure and the lack of skewness.

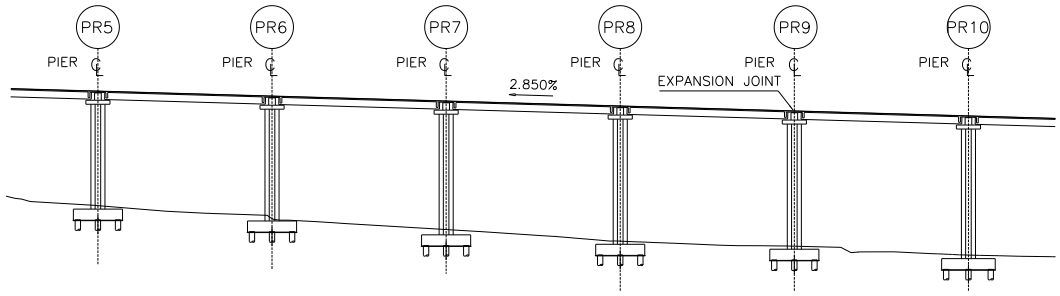

Figure 2-2 Profile View of the Bridge between Pier-5 and Pier-10

The superstructure of the Demirtas Viaduct is composed of 12 pre-tensioned (I) girders with 160 cm depth and 20 cm thick slab. Each girder is seated on the elastomeric bearings. The cross-section of the superstructure and the I-girder are presented in Figure 2-3 and Figure 2-4, respectively. The superstructure rests on a single column bent formed by a cap beam and a single column. The cross-sections

for the cap beam and the column are shown in Figure 2-5 and Figure 2-6, respectively. The columns rest on raft foundations which are further supported by piles on the bottom of the valley. There is a significant amount of reinforcement on the columns. The bottom cross-section of Pier-10 in which reinforcement ratio is 0.02 is given in Appendix A. The elevation view of column cross-section and bridge cross-section is provided in Figure 2-7 and Figure 2-8, respectively. The weight of superstructure for one span and cap beam is 9018 kN and 305.5 kN, respectively. The pier heights and weights with the information of continuity over pier is provided in table 2.2.

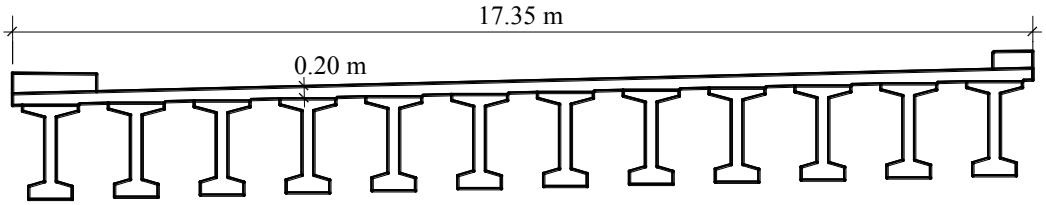

Figure 2-3 Superstructure Cross Section

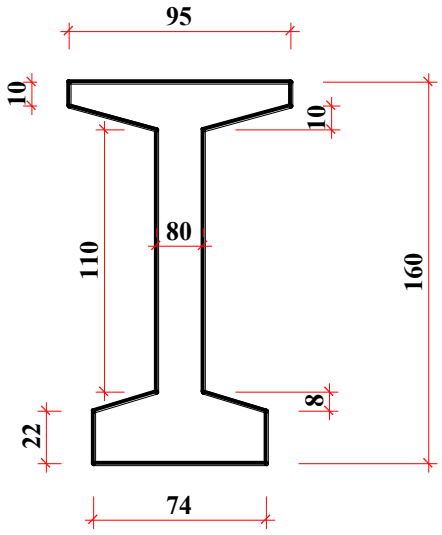

Figure 2-4 I Girder Dimensions (cm)

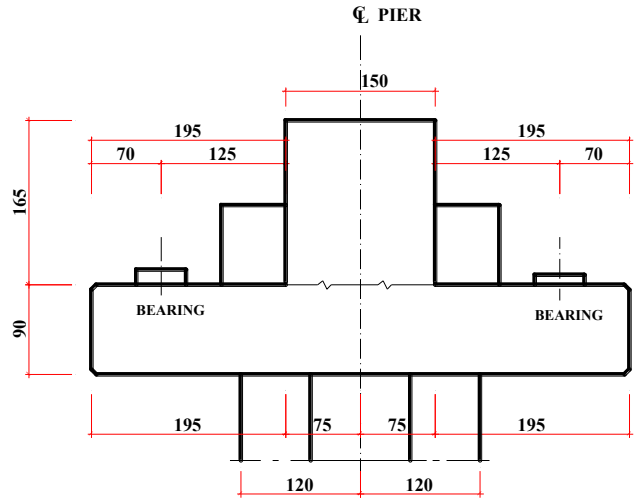

Figure 2-5 Cap Beam Dimensions (cm)

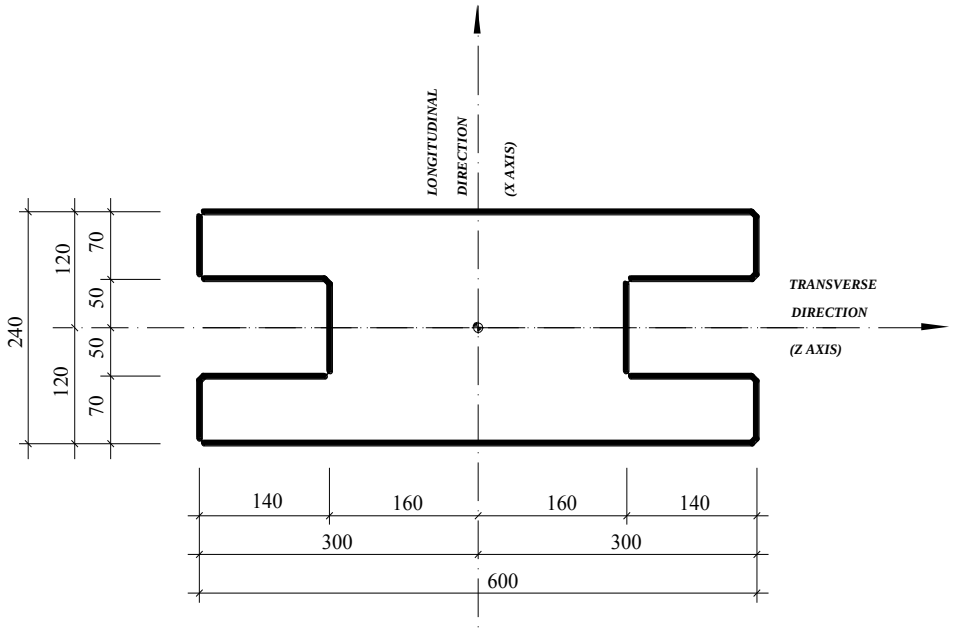

Figure 2-6 Column Cross Section (cm)

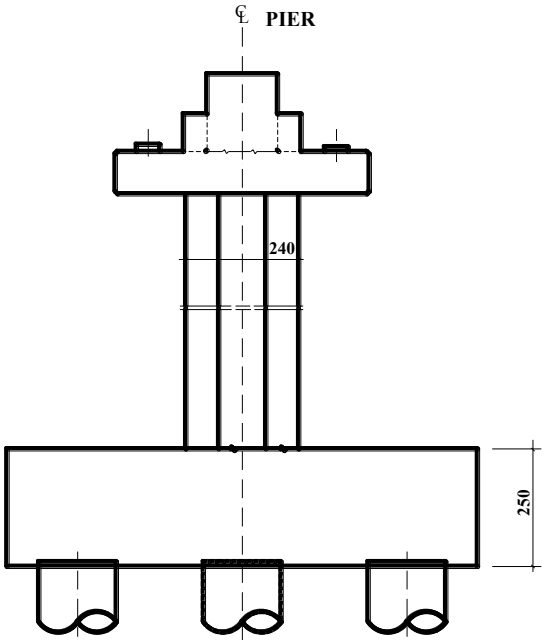

Figure 2-7 Elevation View of Cap-Beam Column Cross Section (cm)

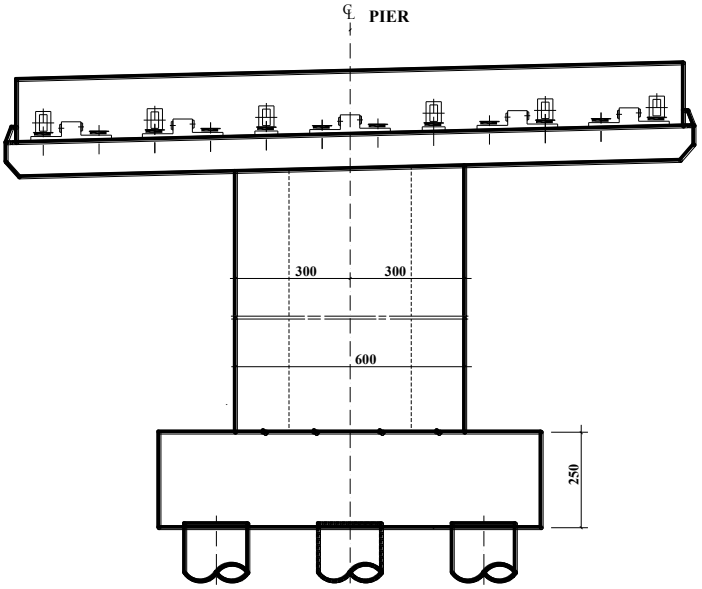

Figure 2-8 Bridge Cross-Section (cm)

Table 2-2 Pier Heights and Weight

Pier	Height (m)	Weight (kN)	Continuity over Pier
1	12.5	3485	yes
2	17	4740	yes
3	19	5297	yes
4	21	5855	no
5	23.5	6552	yes
6	25	6970	yes
7	26	7249	yes
8	27	7528	yes
9	28	7806	no
10	29	8085	yes
11	28	7806	yes
12	28	7806	yes
13	28	7806	yes
14	27	7528	no
15	26	7249	yes
16	25	6970	yes
17	23.5	6552	yes
18	22	6134	yes
19	21	5855	no
20	20	5576	yes
21	19	5297	yes
22	21	5855	yes
23	20	5576	yes
24	17	4740	no
25	17	4740	yes
26	17	4740	yes
27	14	3903	yes

2.3 BRIDGE MODELS

Demirtas Viaduct is a considerably complex structural system comprised of a number of sub-systems connected by expansion joints over the cap-beams. Further complicating the structural system, the roadway is continuous over the expansion joints in effect providing a connection between the independent spans separated by expansion joints. As given above, a number of possible modeling approaches to this complex system is possible. Considering those suggestions, two different bridge models having different number of spans are built. Absent the complete modeling of all 28 spans, the first of these models, model B; correspond to the most complete

model to the system which considers the effect of the side-spans on the mid-span more realistically. The model consists of 15 spans and three different structural systems connected by expansion joints. The second model, model C, consists of 5 segments and the expansion joints and corresponds to the smallest system in which the segment behavior (at the middle of the bridge) can be simulated. Simple illustrations of the models are presented in Figure 2-9.

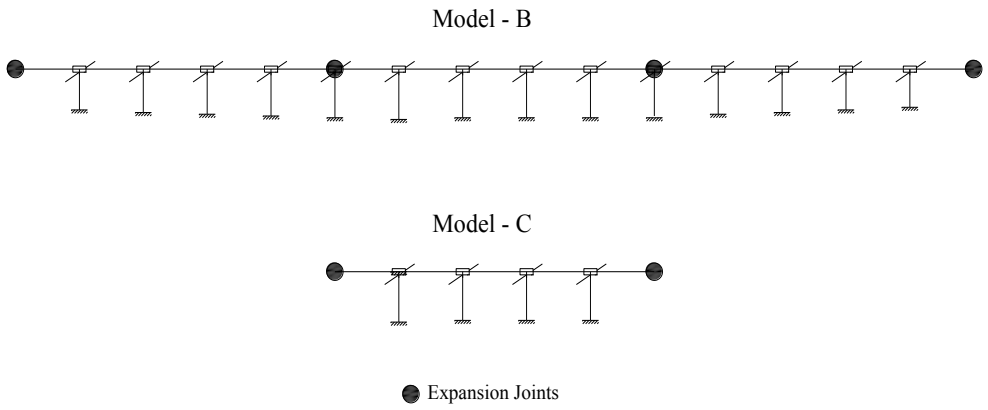

Figure 2-9 Model B and Model C, Elevation View

Expansion joints and beam-column connections form an important part of the simulation models which require a more detailed explanation. The superstructure rests on the cap-beam on elastomeric bearings at each support. While the superstructure girders are separated by the cap beam, they are connected by the roadway as given in the detail in Figure 2-10. A set of rigid elements are employed in the analysis models to represent this geometry. At the expansion joint, each span is separated by a gap around the cap beam which is modeled with the details given in Figure 2-11. The boundary conditions of the superstructure are defined with the equivalent stiffness of the elastomeric components under the girders for all 6 directions. In other words, the stiffness of 12 elastomeric components is reduced to one equivalent spring for each translational and rotational direction. The rotational springs at these connections are obtained for the rigid body rotation of the end of the superstructure on the cap-beam. At pier tops, these springs are located between the cap beam rigid element and superstructure rigid element (Figure 2-10). At the ends of the bridge one end of these springs is linked to the superstructure, and the other

end is fastened to the fixed support. Boundary conditions for the column bases are assumed as fixed supports since pile foundations are present. The cap beam and deck connection details for the piers with and without expansion joints are provided in Appendix A.

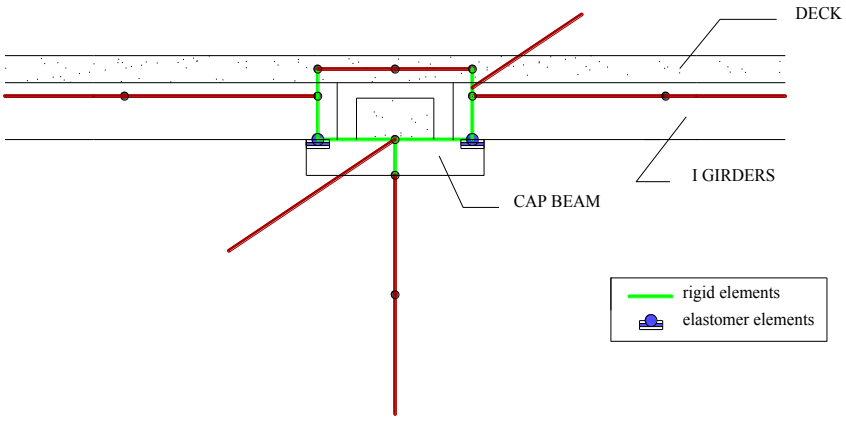

Figure 2-10 Superstructure-Cap Beam-Column Connection

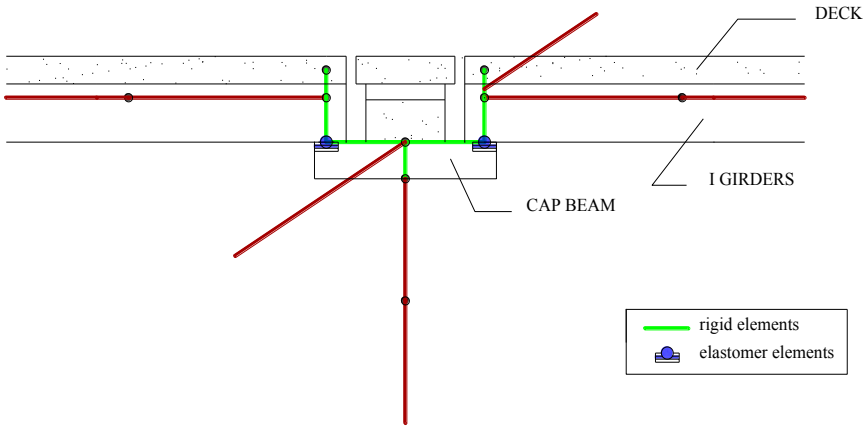

Figure 2-11 Superstructure-Cap Beam-Column Connection at Expansion Joints

2.4 OPEN-SEES MODEL AND ANALYSIS RESULTS

The analytical models for the Demirtas Viaduct are constructed using OpenSees - an object-oriented, open-source software framework. OpenSees is a powerful tool for nonlinear analysis because the element and material definitions as well as the analysis commands are quite comprehensive. In addition, utilizing user defined

elements and materials are possible (Mazzoni et al., 2006). Another advantage of OpenSees is the capability to execute similar analyses sequentially or in an iterative setting much like a coding language. For visualization of the models and post-processing of the results, MATLAB is employed in this study.

Three dimensional beam-column elements are used for the modeling of the Demirtas Viaduct by defining section and material properties. Each span and cap beam is modeled with 8 elements. Columns are divided into 2 m and 3 m elements according to their heights to make sure at least 5 elements are used along the length of the column. Translational masses in three directions are assigned to the nodes considering the tributary lengths of all the elements considered in the analysis. The line element properties such as area, moment of inertia and torsional constant are calculated by both hand calculations and SAP2000 Section Designer tool.

Material properties for different elements of the bridge are provided in Table 2-3. Young's modulus and Shear Modulus are required for the definition of material property for the elastic model. For nonlinear modeling, a material model which is the combination of flexural behavior of the column plastic hinge regions in longitudinal and transverse directions is defined for the column top and bottom portions. However plastic hinges have been obtained only at the bottom of the columns as expected.

Table 2-3 Material Properties

Material Property	Superstructure	Column	Cap Beam
Compressive Strength	40 MPa	25 MPa	25 MPa
Young's Modulus (E_c)	33GPa	26 GPa	26 GPa
Poisson's ratio	0.2	0.2	0.2
Unit mass	2450 kg/m^3	2450 kg/m^3	2450 kg/m^3
Shear Modulus (G_C)	13.7 GPa	10.8 GPa	10.8 GPa

2.4.1 Eigen Value Analyses

The principal modes of the constructed finite element models are presented in Table 2-4. In these analyses, the flexural rigidity of the column cross-sections are assumed at 0.45 of the gross flexural rigidity of the section, and the superstructure flexural rigidity is assumed as 0.60 of the flexural rigidity of the section. The fundamental modes of both systems are longitudinal, corresponding to the superstructure motion on the column in the direction of the motorway (Figure 2-12 and Figure 2-13). Given the dominance of the superstructure motion on this mode and the effect of the flexibility of bearings, this mode shape is usually not characterized as critical for the structural behavior of the system. The first transverse mode, obtained at 1.2 seconds for the Model B, and 1.1 seconds for Model C, is considered as the critical structural mode in the remainder of this study. As given in Table 2-4, the transverse mode in model B and C are very close to each other.

Table 2-4 Fundamental Modes of Bridge Models

Model B						
mode	frequency	period	mode-direction	Mass participation (%)		
				x	y	z
1	0.481	2.078	longitudinal	0.58	2.87E-07	3.31E-10
2	0.59	1.695	longitudinal	0.02	6.50E-06	1.82E-08
3	0.62	1.613	longitudinal	0.17	3.29E-07	7.50E-10
4	0.836	1.196	transverse	3.38E-09	1.31E-05	0.44

Model C						
mode	frequency	period	mode-direction	Mass participation (%)		
				x	y	z
1	0.567	1.763	longitudinal	0.79	6.58E-07	1.02E-09
2	0.916	1.092	transverse	1.17E-09	1.81E-05	0.70

In order to carry out MPS procedure, the modal period and the mode shape are required while the natural period of the structure is the only necessary parameter for ASCE scaling.

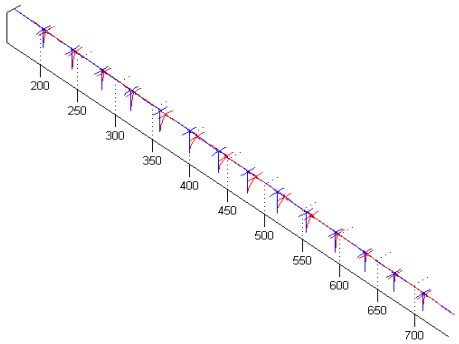	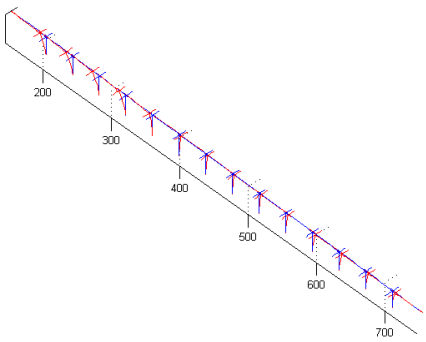
Mode 1	Mode 2
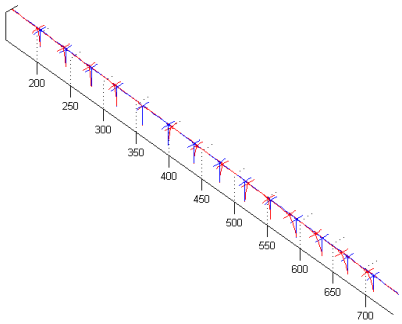	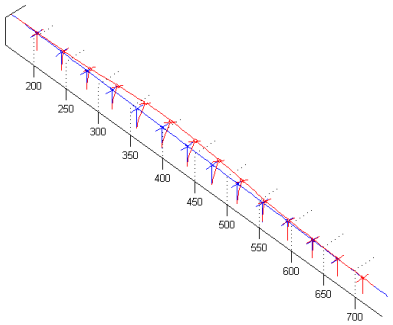
Mode 3	Mode 4

Figure 2-12 Mode Shapes for Model B

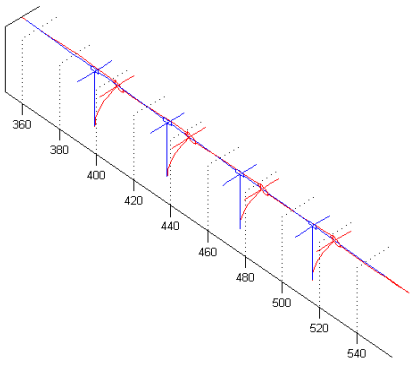	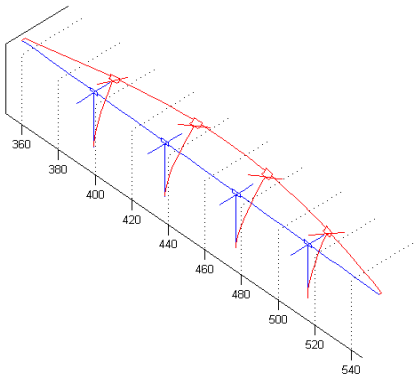
Mode 1	Mode 2

Figure 2-13 Mode Shapes for Model C

2.4.2 Push-Over Analysis

The non-linearity is assumed on the column elements in this study by defining possible plastic hinge regions at the top and bottom parts of the columns. Columns are modeled with "beam with hinges" element which includes plastic hinge zones at two ends of the element and elastic portion at the middle of the element. The plastic hinge lengths are calculated according to the CALTRANS SDC 1.7 specification using the formula given below.

$$L_P = 0.08L + 0.022 f_{ye} d_{bl} \geq 0.044 f_{ye} d_{bl} \quad (2\text{-}1)$$

L: Column length from the point of maximum moment to the point of contra-flexure (mm)

f_{ye}: Expected yield stress of reinforcement

d_{bl}: Nominal bar diameter of longitudinal column reinforcement

The heights of each pier and the corresponding plastic hinge lengths are provided in the Table 2-5.

Table 2-5 Pier Heights and Plastic Hinge Lengths

Pier	Height (m)	Plastic Hinge Length (m)
5	23.5	2.21
6	25	2.33
7	26	2.41
8	27	2.49
9	28	2.57
10	29	2.65
11	28	2.57
12	28	2.57
13	28	2.57
14	27	2.49
15	26	2.41
16	25	2.33
17	23.5	2.21
18	22	2.09

The inelastic properties of the plastic hinges are determined according to the moment-curvature analysis of the column section at the base. Moment curvature

analysis of the column section is carried out utilizing both SAP2000 (2011) and UCFYBER (1999): similar results are obtained. The column section modeled in SAP2000 is provided in Figure 2-14.

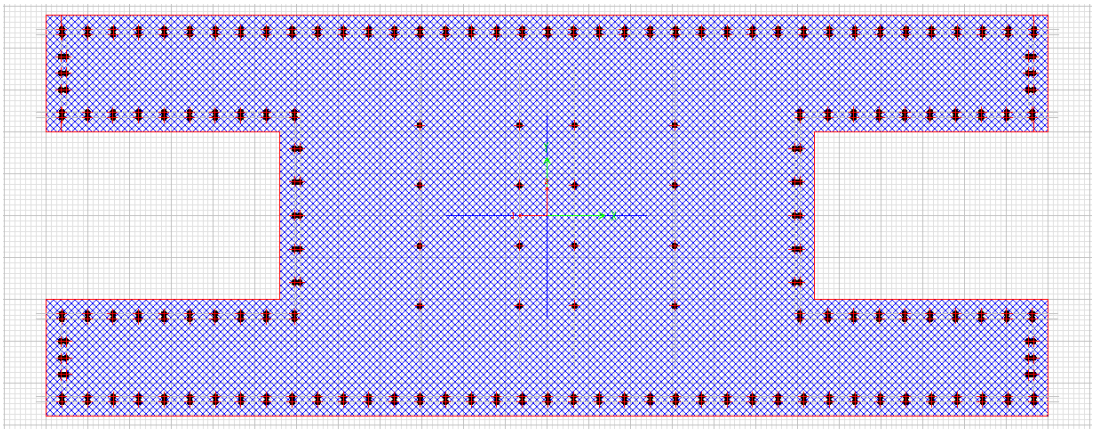

Figure 2-14 Column Section for Moment-Curvature Analysis

Although reinforcement detailing of columns show differences from each other, for simplicity the bottom cross-section of one column (Pier-10) is used to obtain moment-curvature relation. Since the stirrups do not make a complete tour around the longitudinal reinforcement in this very large column, the core concrete is assumed as unconfined. The stress-strain behavior of the unconfined concrete and reinforcement are presented in Figure 2-15**.**

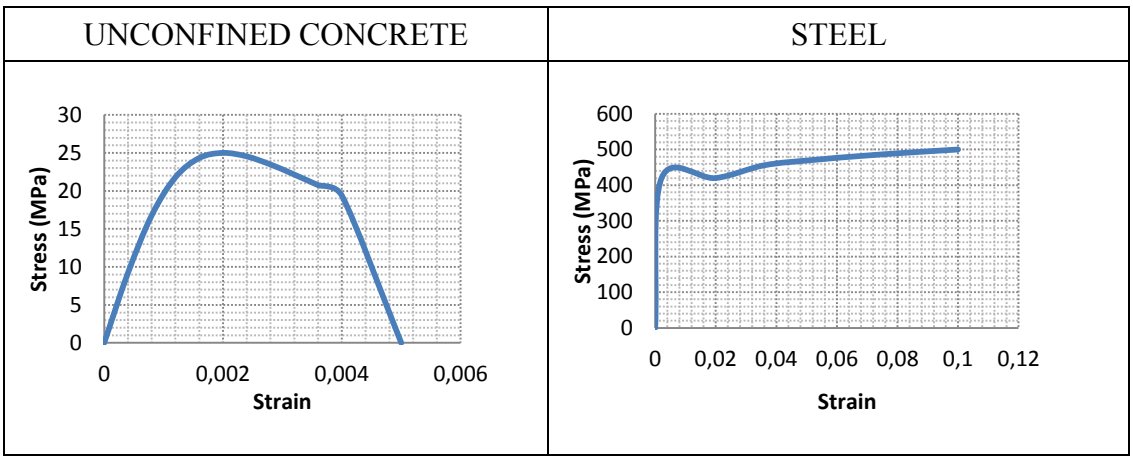

Figure 2-15 Stress-Strain Behavior, Unconfined Concrete and Steel

Moment curvature results obtained from SAP2000 are provided in Figure 2-16. Strain hardening of steel is considered for moment capacity computation. In the transverse direction, moment capacity of the section is obtained approximately as 225000 kNm while in the longitudinal direction the capacity is obtained as 100000 kNm (The computed strength corresponds to ultimate capacity of the section given that characteristic strength of concrete and overstrength capacity of steel is used). According to the given moment-curvature relations, displacement ductility capacity for Pier-10 is computed as 1.85 and 2.4 in transverse and longitudinal directions, respectively.

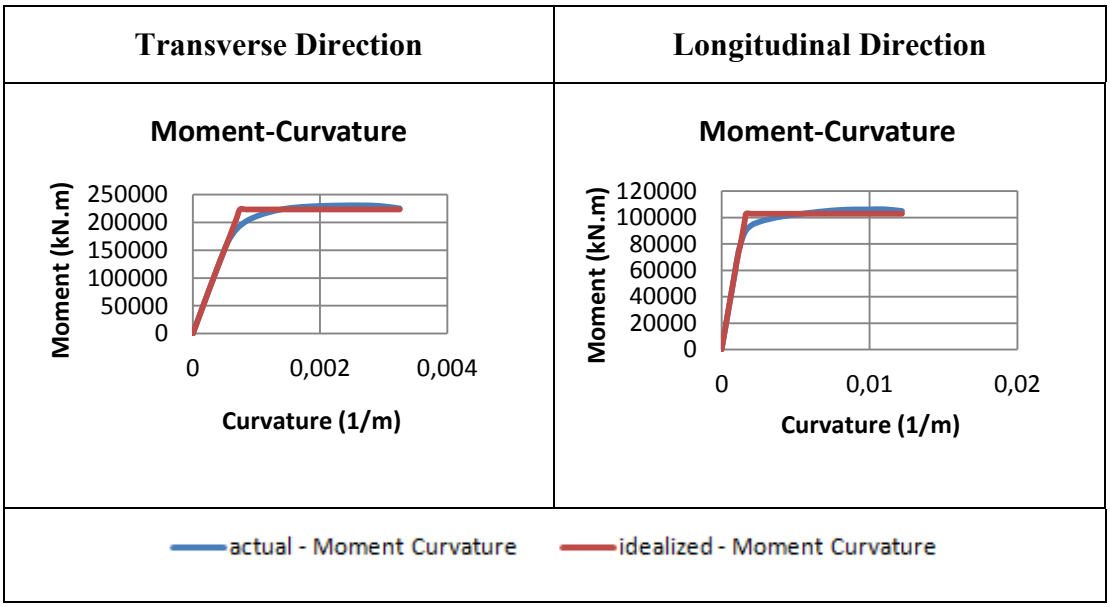

Figure 2-16 Moment Curvature Diagrams for Transverse and Longitudinal Direction

Drift limit is estimated from moment curvature equations according to the procedure in section 3.1.3 in SDC 1.7 (CALTRANS, 2013). The drift limit for Pier-10 in transverse direction is computed as 1.35% and displacement capacity is obtained as 39 cm. From pushover analysis, displacement capacity for the same pier is obtained as 37 cm.

2.4.3 Non-Linear Time History Analysis

Nonlinear transient analyses are performed for the two models, Model B and C, with the scaled and the unscaled motions. Transient analyses are conducted using the uniform support excitation feature in Open-Sees with 0.005 second time-stepping interval. Newmark average acceleration method is used as the time stepping scheme in the analysis. Damping for the bridge models is defined as Rayleigh damping by determining the coefficients α and β ensuring the damping close to 0.05 for the first longitudinal and transverse modes.

The displacement and acceleration time histories of important locations on the models are recorded. The base shear and moment time history for all the bents are obtained. Sample time histories for the displacement and acceleration at the top of bent-10 for the 2475-year event (model B, motion-25), is shown in Figure 2-17. The corresponding base moment and shear at the base of the column is presented in Figure 2-18.

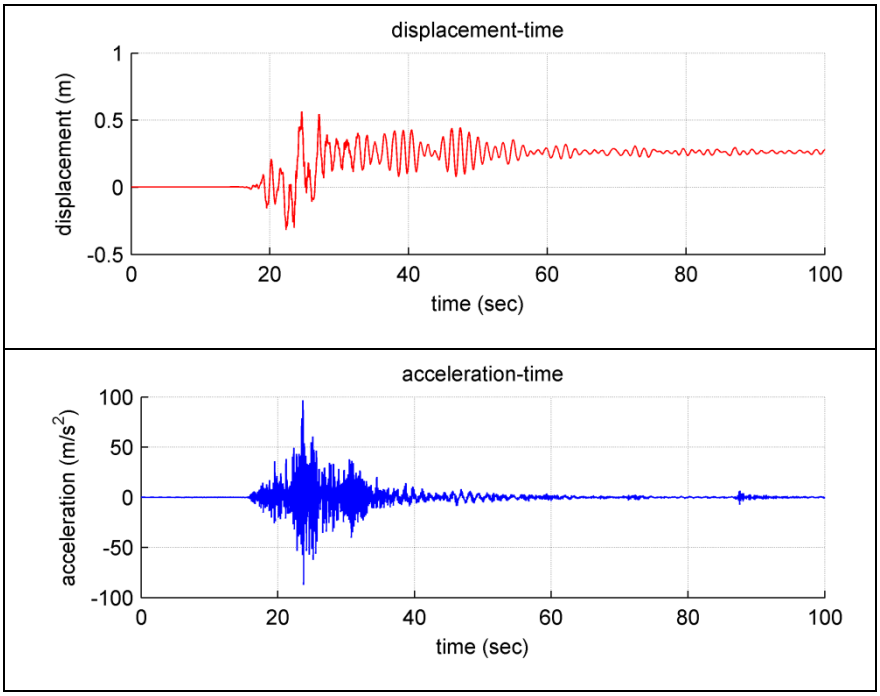

Figure 2-17 Displacement and Acceleration Time History, Bent 10

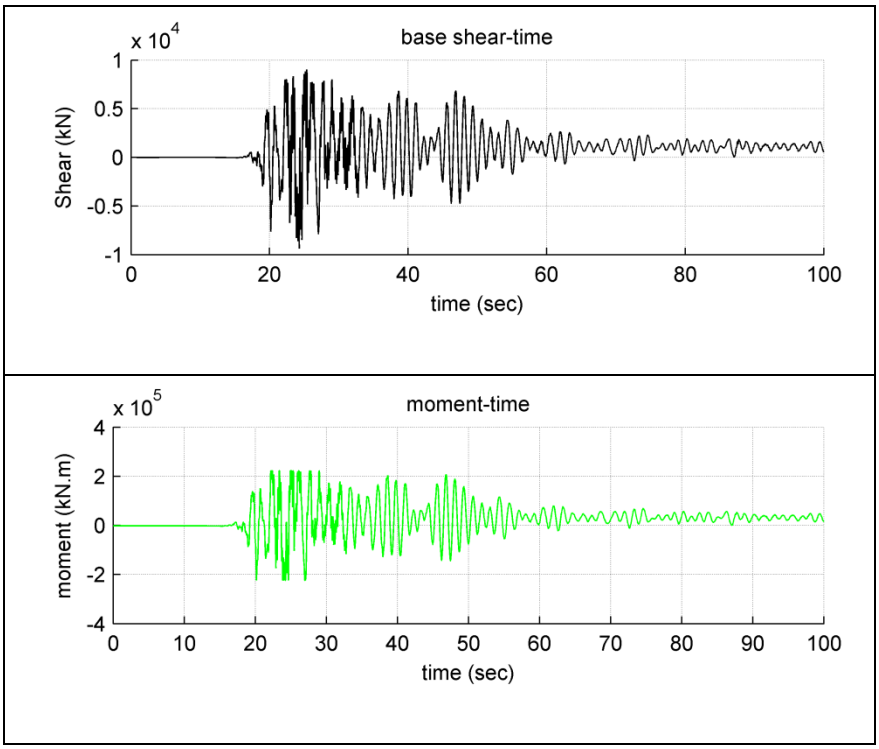

Figure 2-18 Base Moment and Base Shear Time History, Bent 10

CHAPTER 3

THE SELECTION AND SCALING OF GROUND MOTIONS FOR USE IN THE NONLINEAR TIME HISTORY ANALYSES OF BRIDGES

3.1 GROUND MOTION SELECTION

The ground motions for seismic design or evaluation are chosen based on the magnitude of the event, distance to the fault and the local soil conditions. The motions, hence selected, should be from former events with similar magnitudes, fault distance and local soil conditions. In order to evaluate the effect of ground motion selection on the analysis of a typical highway bridge subjected to high seismic hazard, the following criteria were chosen for the selection of the ground motions in this study:

- Moment magnitude (M_w) between 6.5 and 7.9
- Maximum 12 km distance to the causative fault and
- $V_{s,30}$ values between 300 and 400 m/s.

Soil condition at a given site is often decided based on the shear wave velocity measurement at the first 30 m below the site, $V_{s,30}$. For the Demirtas Viaduct, $V_{s,30}$ was measured as 350 m/s (TÜBİTAK, KAMAG 110G093). Considering the criteria given above, 35 different ground motions are chosen from the PEER Strong Motion Database. Each ground motion consists of two horizontal and one vertical components of acceleration time history. For analyses, one of the two recordings in horizontal direction is utilized. The list of the selected ground motions and the corresponding features are given in Table 3-1. The acceleration time series of the motions are shown in Figure 3-1.

The selected ground motions are divided into 5 sets of 7 each to form the ground motion groups for scaling purposes. While grouping the records, care was taken not to put more than two records obtained from the same event into the same set in order

to avoid the dominance of a single event in the set (Reyes et al., 2012). Except for this criterion, ground motion sets are constituted randomly. The ground motion sets are given in Table 3-2 to Table 3-6.

Table 3-1 Ground Motion Records Used in the Analyses

ID #	Event	Mw	Mechanism	PGA (g)	Rjb(km)	Rrup(km)	Vs30(m/s)	Station	H1 Acc. File Name
1	Superstition Hills-02	6.54	strike slip	0.432	0.95	0.95	348.69	Parachute Test Site	SUPER.B_B-PTS225.AT2
2	Superstition Hills-02	6.54	strike slip	0.582	5.61	5.61	362.38	Superstition Mtn Camera	SUPER.B_B-SUP045.AT2
3	Loma Prieta	6.93	Reverse Oblique	0.514	7.58	8.5	380.89	Saratoga - Aloha Ave	LOMAP_STG000.AT2
4	Loma Prieta	6.93	Reverse Oblique	0.258	8.48	9.31	347.9	Saratoga - W Valley Coll.	LOMAP_WVC000.AT2
5	Erzican, Turkey	6.69	strike slip	0.387	0	4.38	352.05	Erzincan	ERZINCAN_ERZ-NS.AT2
6	Northridge-01	6.69	Reverse	0.411	0	5.43	373.07	Jensen Filter Plant Administrative Building	NORTHR_JEN022.AT2
7	Northridge-01	6.69	Reverse	0.753	0	8.44	380.06	LA - Sepulveda VA Hospital	NORTHR_SPV270.AT2
8	Northridge-01	6.69	Reverse	0.557	5.54	7.46	325.67	Pardee - SCE	NORTHR_PAR--L.AT2
9	Northridge-01	6.69	Reverse	0.853	0	5.19	370.52	Sylmar - Converter Sta East	NORTHR_SCE011.AT2
10	Kobe, Japan	6.9	strike slip	0.834	0.94	0.96	312	KJMA	KOBE_KJM000.AT2
11	Kobe, Japan	6.9	strike slip	0.697	0	0.27	312	Takarazuka	KOBE_TAZ000.AT2
12	Chi-Chi, Taiwan	7.62	Reverse Oblique	0.160	7.64	7.64	350.06	TCU051	CHICHI_TCU051-E.AT2
13	Chi-Chi, Taiwan	7.62	Reverse Oblique	0.239	6.34	6.34	359.13	TCU055	CHICHI_TCU055-E.AT2
14	Chi-Chi, Taiwan	7.62	Reverse Oblique	0.201	8.51	8.51	375.42	TCU060	CHICHI_TCU060-E.AT2
15	Chi-Chi, Taiwan	7.62	Reverse Oblique	0.790	0.57	0.57	305.85	TCU065	CHICHI_TCU065-E.AT2
16	Chi-Chi, Taiwan	7.62	Reverse Oblique	0.212	2.11	2.11	389.41	TCU101	CHICHI_TCU101-E.AT2
17	Duzce, Turkey	7.14	strike slip	0.119	9.14	9.14	338	Lamont 1062	DUZCE_1062-N.AT2

Table 3-1 Ground Motion Records Used in the Analyses (Continued)

ID #	Event	Mw	Mechanism	PGA (g)	Rjb(km)	Rrup(km)	Vs30(m/s)	Station	H1 Acc. File Name
18	Denali, Alaska	7.9	strike slip	0.333	0.18	2.74	329.4	TAPS Pump Station #10	DENALI_PS10-047.AT2
19	Tottori, Japan	6.61	strike slip	0.940	0.83	0.97	310.21	TTRH02	TOTTORI_TTRH02NS.AT2
20	San Simeon, CA	6.52	Reverse	0.179	6.97	7.25	362.42	Cambria - Hwy 1 Caltrans Bridge	SANSIMEO_37737090.AT2
21	Niigata, Japan	6.63	Reverse	1.167	0.21	9.88	372.33	NIG019	NIIGATA_NIG019NS.AT2
22	Niigata, Japan	6.63	Reverse	0.533	7.45	8.47	331.63	NIG020	NIIGATA_NIG020NS.AT2
23	Niigata, Japan	6.63	Reverse	0.464	6.27	8.93	375	NIGH11	NIIGATA_NIGH11NS.AT2
24	Montenegro, Yugoslavia	7.1	Reverse	0.293	3.97	5.76	318.74	Ulcinj - Hotel Olimpic	MONTENE.GRO_ULO000.AT2
25	Iwate, Japan	6.9	Reverse	0.905	5.97	6.02	371.06	IWTH26	IWATE_IWTH26NS.AT2
26	Darfield, New Zealand	7	strike slip	0.764	1.22	1.22	344.02	GDLC	DARFIELD_GDLCN55W.AT2
27	Darfield, New Zealand	7	strike slip	0.450	7.29	7.29	326.01	HORC	DARFIELD_HORCN18E.AT2
28	Irpinia, Italy-01	6.9	Normal	0.227	6.78	10.84	382	Sturno (STN)	ITALY_A-STU000.AT2
29	Loma Prieta	6.93	Reverse Oblique	0.285	10.27	10.97	308.55	Gilroy - Historic Bldg.	LOMAP_GOF160.AT2
30	Landers	7.28	strike slip	0.274	11.03	11.03	379.32	Joshua Tree	LANDERS_JOS000.AT2
31	Chi-Chi, Taiwan	7.62	Reverse Oblique	0.592	0	10.97	363.99	TCU079	CHICHI_TCU079-E.AT2
32	Chuetsu-oki, Japan	6.8	Reverse	0.303	9.43	11.94	383.43	Joetsu Kakizakiku Kakizaki	CHUETSU_65010NS.AT2
33	Chuetsu-oki, Japan	6.8	Reverse	0.357	0	11.75	338.32	Kawanishi Izumozaki	CHUETSU_65039NS.AT2
34	Iwate, Japan	6.9	Reverse	0.260	5.09	11.12	398.59	MYGH02	IWATE_MYGH02NS.AT2
35	Darfield, New Zealand	7	strike slip	0.472	11.86	11.86	344.02	DFHS	DARFIELD_DFHSS17E.AT2

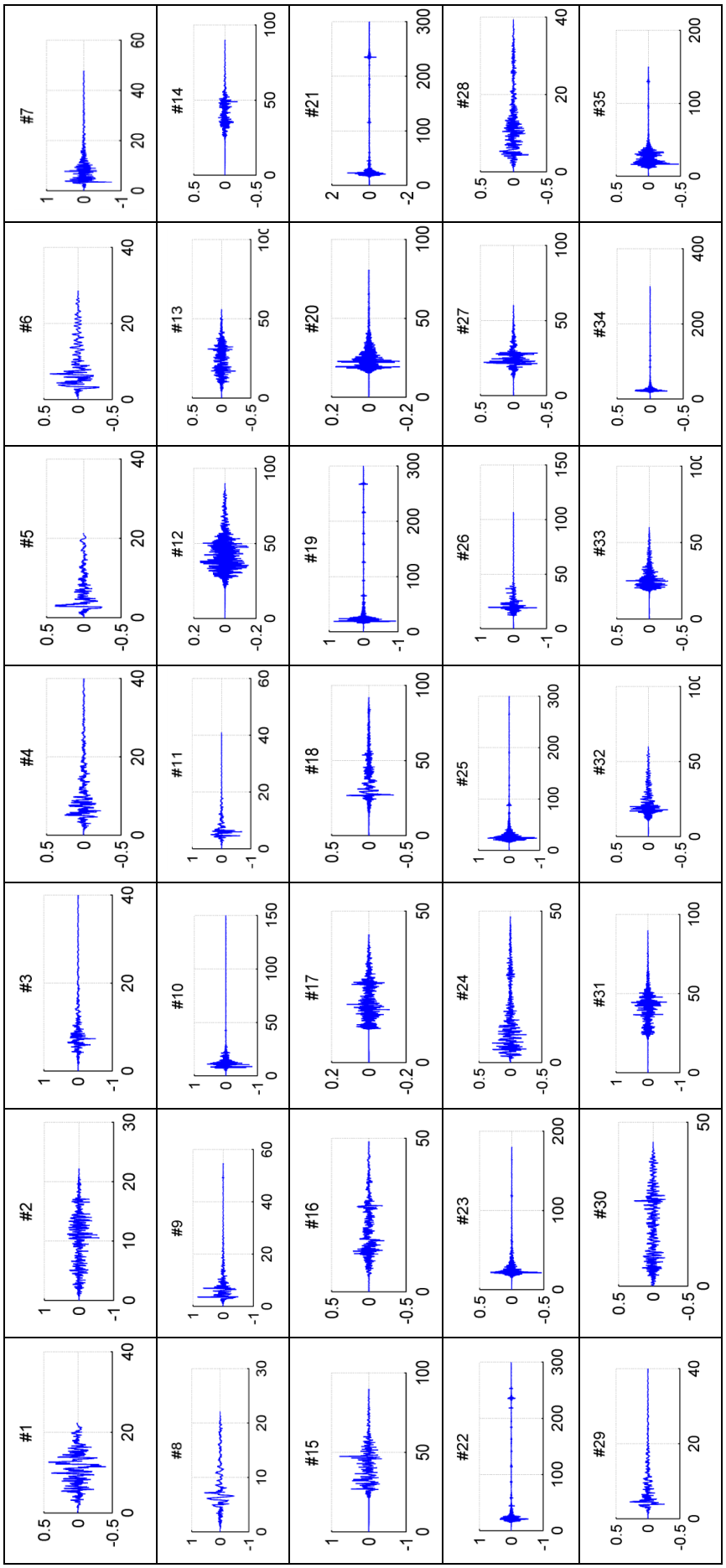

Figure 3-1 Acceleration Time Histories of Selected Motions

Table 3-2 Ground Motion Records - Set-1

ID	Event	Mw	Mechanism	PGA (g)	V_{s30} (m/s)
1	Superstition Hills-02	6.54	strike slip	0.432	348.7
3	Loma Prieta	6.93	Reverse Oblique	0.514	380.9
5	Erzican, Turkey	6.69	strike slip	0.387	352.1
6	Northridge-01	6.69	Reverse	0.411	373.1
10	Kobe, Japan	6.9	strike slip	0.834	312.0
12	Chi-Chi, Taiwan	7.62	Reverse Oblique	0.160	350.1
13	Chi-Chi, Taiwan	7.62	Reverse Oblique	0.239	359.1

Table 3-3 Ground Motion Records - Set-2

ID	Event	Mw	Mechanism	PGA (g)	V_{s30} (m/s)
2	Superstition Hills-02	6.54	strike slip	0.582	362.4
4	Loma Prieta	6.93	Reverse Oblique	0.258	347.9
7	Northridge-01	6.69	Reverse	0.753	380.1
11	Kobe, Japan	6.9	strike slip	0.697	312.0
14	Chi-Chi, Taiwan	7.62	Reverse Oblique	0.201	375.4
17	Duzce, Turkey	7.14	strike slip	0.119	338.0
18	Denali, Alaska	7.9	strike slip	0.333	329.4

Table 3-4 Ground Motion Records - Set-3

ID	Event	Mw	Mechanism	PGA (g)	V_{s30} (m/s)
8	Northridge-01	6.69	Reverse	0.557	325.7
15	Chi-Chi, Taiwan	7.62	Reverse Oblique	0.790	305.9
20	San Simeon, CA	6.52	Reverse	0.179	362.4
21	Niigata, Japan	6.63	Reverse	1.167	372.3
24	Montenegro, Yugoslavia	7.1	Reverse	0.293	318.7
25	Iwate, Japan	6.9	Reverse	0.905	371.1
31	Chi-Chi, Taiwan	7.62	Reverse Oblique	0.592	364.0

Table 3-5 Ground Motion Records - Set-4

ID	Event	Mw	Mechanism	PGA (g)	V_{s30} (m/s)
9	Northridge-01	6.69	Reverse	0.853	370.5
16	Chi-Chi, Taiwan	7.62	Reverse Oblique	0.212	389.4
22	Niigata, Japan	6.63	Reverse	0.533	331.6
26	Darfield, New Zealand	7	strike slip	0.764	344.0
30	Landers	7.28	strike slip	0.274	379.3
32	Chuetsu-oki, Japan	6.8	Reverse	0.303	383.4
34	Iwate, Japan	6.9	Reverse	0.260	398.6

Table 3-6 Ground Motion Records - Set-5

ID	Event	Mw	Mechanism	PGA (g)	V_{s30} (m/s)
19	Tottori, Japan	6.6	strike slip	0.940	310.2
23	Niigata, Japan	6.6	Reverse	0.464	375.0
27	Darfield, New Zealand	7	strike slip	0.450	326.0
28	Irpinia, Italy-01	6.9	Normal	0.227	382.0
29	Loma Prieta	6.9	Reverse Oblique	0.285	308.6
33	Chuetsu-oki, Japan	6.8	Reverse	0.357	338.3
35	Darfield, New Zealand	7	strike slip	0.472	344.0

3.2 TARGET EARTHQUAKE SPECTRA

As indicated in the previous sections, for the comparison of scaling methods, only mean spectrum of a large group of earthquake records have been utilized in the past (Kalkan et al., 2010 ,2012). In this study, along with a mean spectrum, target hazard spectra from two design codes, (AASHTO-2010 and DLH 2007) are also used as the seismic guidelines from these codes are commonly used for design of highways in Turkey. In fact, AASHTO 2010 and DLH design spectra yield almost the same spectral shapes with the same short and long period spectral acceleration coefficients. The mean spectrum used in the analyses corresponds to a lower seismic hazard condition, i.e. an Operation Based Event (OBE). In order to obtain a comparison basis for higher levels, a 1000 year return period event from AASHTO (2010) is used as the Maximum Design Event (MDE). The 2475-year return period event used from the DLH recommendations is chosen to be the Maximum Characteristic Event

(MCE) at the site. The target spectra used in the study are explained in the following headings.

3.2.1 OBE Level Spectrum

Geometric mean of the 5% damped acceleration spectrum of the 35 ground motions is chosen as the OBE level target spectra in this study. The use of the geometric mean spectrum in this fashion is preferred to be able to compare the results with previous studies in which such an approach was used as the target spectrum to compare the scaling methodologies. The acceleration response spectra of the 35 motions and their geometric mean, the target spectrum, are presented in Figure 3-2.

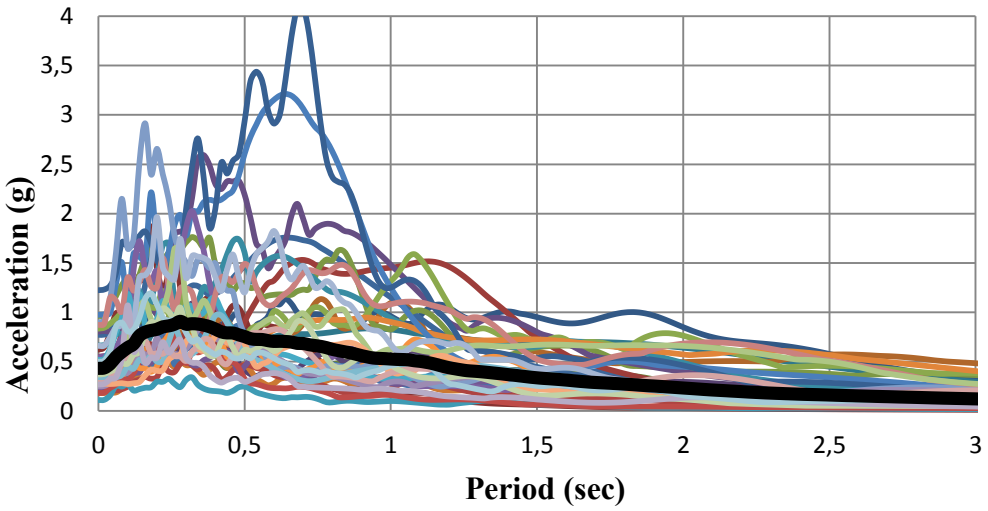

Figure 3-2 Geometric Mean Spectrum of Selected Records

3.2.2 MDE Level Spectrum - AASHTO (2010)

The 1000 year return period event from AASHTO (2010) is chosen as the MDE level demand based on the ground conditions at the site. The coefficients and the equations necessary to obtain the AASHTO (2010) design spectrum are given in Figure 3-3.

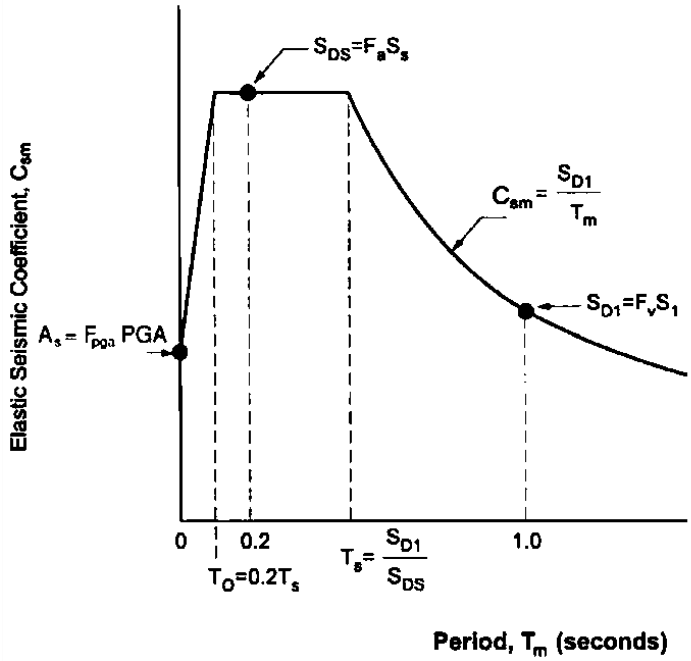

Figure 3-3 AASHTO (2010) Design Spectrum

As shown in the Figure 3-3, the peak ground acceleration (PGA), short period spectral acceleration (S_s), long period spectral acceleration (S_l) and their corresponding coefficients F_{pga}, F_a and F_v are the required parameters to obtain the AASHTO (2010) design spectrum. Among these parameters, the peak ground acceleration (PGA), short period spectral acceleration (S_s) and long period spectral acceleration (S_l) depend on the seismic hazard at a site and are determined from the seismic hazard maps or from site specific hazard analysis. The F_{pga}, F_a and F_v factors corresponding to a probability of seven percent exceedance in 75 years which corresponds to an event with 1000-year return period are chosen based on the site class from the respective tables in AASHTO (2010). PGA, S_s and S_l coefficients for the 1000-year return period earthquake event are determined from the data obtained for the TUBITAK 110G093 project for the Demirtas site (TÜBİTAK, KAMAG 110G093). The site condition is determined according to the $V_{s,30}$ value of the site which corresponds to the site class D in AASHTO (2010) (Mestav, 2014).

3.2.3 MCE Spectrum - DLH

The 2475 year return period event from DLH (2007) is chosen as the MCE level demand based on the ground conditions at the site. DLH design spectrum is also often used for the design of highway bridges in Turkey. The suggested equations are almost the same with AASHTO (2010) Design Spectrum: the seismic hazard parameters (S_s and S_l) are taken from the tables or the maps provided in the DLH document. DLH equations are used to get the third target spectrum.

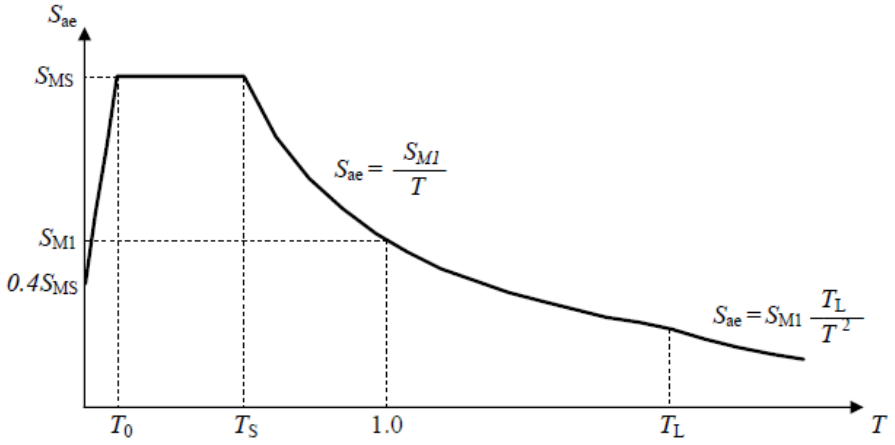

Figure 3-4 General Form of DLH Design Spectrum

Similar to the AASHTO (2010) design spectrum equations, to obtain the DLH spectrum, seismic hazard parameters (S_s and S_l) and their related site coefficients (F_a and $F_{v)}$ should be determined. Values for S_s and S_l are provided in DLH specification for three earthquake levels which are the events with return periods 72 years (D1), 475 years (D2) and 2475 years (D3). These coefficients can be found from the maps or the tables constituted according to latitude and longitude coordinates. The spectrum obtained by using the coefficients for the coordinates of Demirtas site at 2475-year earthquake level does not make a very significant difference with the spectrum at the lower earthquake level, (MDE). In order to increase the target level significantly, the hazard at a site located on the longitude 36.4º and latitude 40.6º is used. In this fashion, the target levels are obtained at R levels of 1, 2 and 3 for the (OBE), (MDE) and (MCE) earthquakes, respectively.

The three different target spectra selected to signify different hazard levels for the Viaduct are presented in Figure 3-5. These spectra are going to be used for ground motion scaling in the next section.

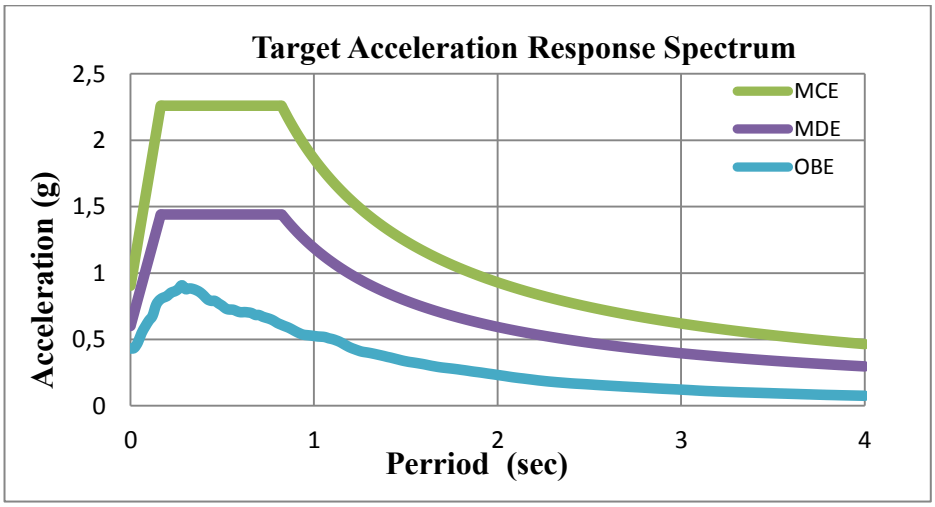

Figure 3-5 Target Spectra

3.3 SCALING OF THE GROUND MOTIONS

In this study, the performance of the ASCE-7-10 (ASCE) Scaling Procedure and Modal Pushover Based Scaling Procedure (MPS) are investigated using the 35 selected motions at three different hazard levels. The scaling methodologies are amplitude based, i.e. the modification to the ground motions are obtained only in terms of linear factors preserving the frequency and pulse content of the motion. Each methodology is shortly summarized in the following sections and the corresponding scale factors, obtained at the different hazard levels, are provided.

3.3.1 ASCE (2010) Scaling

ASCE/SEI scaling procedure recommends the scaling of the selected records such that the mean spectrum of the scaled records are greater than the target spectrum in the range between 0.2 T_n and 1.5 T_n where T_n is the natural period of the structure. Due to the nature of the scaling process, scale factors are not unique, i.e. the motions in the group can be scaled in many different alternatives satisfying the scaling

criteria. In this study, the ASCE scaling factors are calculated using the algorithm provided by Reyes et al. (2014), developed to obtain the scale factors close to unity.

Two different scale factors, SF_1 and SF_2, are computed in this procedure. The first scaling factor (SF_1) is obtained for each record by minimizing the difference between the target spectrum and the 5% damped response spectrum of the motions for the range of $0.2T_n$ -$1.5T_n$. SF_1 factors for each motion are obtained by solving the Equation 3-1 given below. The SF_1 scale factor modifies the response spectrum of the motion to be as close to the target spectrum as possible (Reyes. et. al, 2014).

$$SF_1 = \min_{0.2T_n \le T \le 1.5T_n} \left(\frac{A_{target} * A_{record}}{A_{record}^{\,2}} \right) \quad \textbf{(3-1)}$$

A_{target} : Acceleration vector of the target response spectrum for $0.2T_n$-$1.5\ T_n$
A_{record} : Acceleration vector of the response spectrum of the motions for $0.2T_n$-$1.5\ T_n$

After the SF_1 values are computed for each record, the SF_2 factors are estimated for the group of motions considered. The SF_2 factor modifies the mean spectra of the records in the group in order to ensure the acceleration values of the mean spectra of the modified set are greater than the target spectrum. All motions are multiplied by the same factor SF_2 at this stage to increase the mean. SF_2 scale factors are estimated with the help of the Equations 3.2 and 3.3 (Reyes et al., 2014).

$$\varepsilon_{ASCE} = \max_{0.2T_n \le T \le 1.5T_n} \left(\frac{A_{target} * A_{scaled,mean}}{A_{scaled}} \right) \quad \textbf{(3-2)}$$

$$SF_2 = (1 - \varepsilon_{ASCE})^{-1} \quad \textbf{(3-3)}$$

The final scale factor for each record is found with the multiplication of SF_1 and SF_2 factors. The illustration of SF_1 and SF_2 scaled response spectrum is given in Figure 3-6 and Figure 3-7.

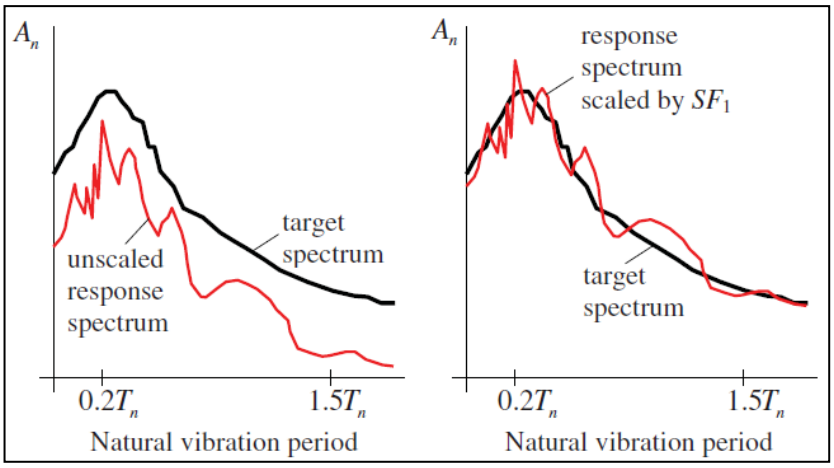

Figure 3-6 SF_1 Scaled Response Spectrum (Adopted from Reyes et al., 2014)

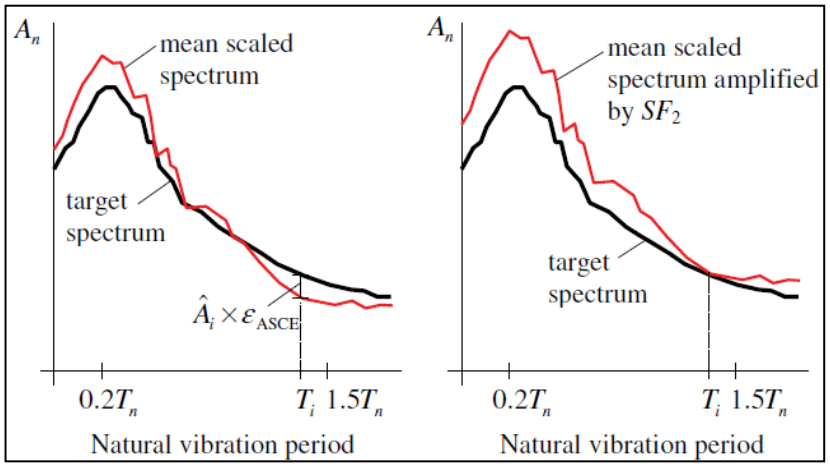

Figure 3-7 SF_2 Scaled Response Spectrum (Adopted from Reyes et al., 2014)

3.3.2 Modal Pushover Based Scaling Method

In the modal pushover based scaling (MPS) method, the scale factors for the time history analysis of the structure are obtained from the analysis of the first mode inelastic SDOF system of the structure with scaled earthquake records. The scale factor used in the analysis of inelastic SDOF system which gives the displacement close enough to the target inelastic displacement is selected as the scale factor for the ground motion considered.

The fundamental property of this method is to incorporate the capacity of the structure in the determination of the scale factors by carrying out inelastic modal pushover analysis (Kalkan et al., 2012).The modal pushover based scaling (MPS) method is proper for the first mode dominated structures and the procedure is extended for the structures in which higher mode contributions are in considerable level (Kalkan et al., 2010). In this study first mode application is found sufficient. Although transverse mode in each bridge model is not seen in the first mode, transverse modes of the bridges are considered in the application of this scaling procedure since transverse mode is considered as the critical mode.

The target inelastic displacement forms an important part of this approach given that it also corresponds to a performance based approach to the design that is somewhat different than the general design methodology based on the response spectrum approach. Given the overwhelming presence of the design spectrums for defining the seismic hazard at the site, for the determination of the target inelastic displacement, the first alternative is calculating the elastic first mode deformation by using an elastic response spectrum and then multiplying the elastic deformation with the inelastic deformation ratio C_R which is estimated from an empirical equation. The elastic response spectrum can be selected as the response spectrum in design specifications which is compatible with the site conditions of the structure. Probabilistic seismic hazard analysis based uniform hazard response spectrum or the mean spectrum of a large group of unscaled ground motions which are appropriate to the seismic hazard situation of the site can also be used (Kalkan et al., 2012).

The second alternative to compute the inelastic target displacement is to use the mean value obtained from the analysis of inelastic SDOF with unscaled motions as the target displacement demand. However, this approach requires a set of unscaled motions fitting the target spectrum at a site which correspond to a set of probable motions that can be observed at the site which lead to realistic displacement demands. Given that the hazard is typically given in terms of location and site condition based spectra, and usually in terms of a uniform hazard response spectrum which forms the aggregation of the hazard at the site due to multiple faults, it is clear that such an approach is not very feasible with today's ground motion data.

In this study, the elastic and inelastic target deformations of the first-mode SDOF system is computed with the help of the equations from 3-4 and 3-5 using the target spectra chosen at different hazard levels.

$$\bar{D} = \frac{\left(T/2\pi\right)^2}{\bar{A}} \quad (3\text{-}4)$$

$$\bar{D}^I = C_R \bar{D} \quad (3\text{-}5)$$

where $\bar{D}$ is the target elastic deformation, $\bar{D}^I$ is target inelastic deformation, T is the elastic natural period, $\bar{A}$ is the target pseudo-spectral acceleration and C_R is the ratio of peak deformations of inelastic and corresponding elastic SDOF systems with known yield-strength reduction factor. C_R ratio is determined from the following formula (Chopra et al., 2004):

$$C_R = 1 + \left[(L_R - 1)^{-1} + \left(\frac{a}{R_y^b} + c\right)\left(\frac{T}{T_c}\right)^d\right]^{-1} \quad (3\text{-}6)$$

in which the L_R is given as:

$$L_R = \frac{1}{R_y}\left(1 + \frac{R_y - 1}{\alpha}\right) \quad (3\text{-}7)$$

where α is the post yield stiffness ratio, T_c is the period separating the acceleration- and velocity -sensitive regions and the parameters are a=61, b=2.4, c=1.5 and d=2.4.

For the estimation of inelastic target displacement with C_R factor, yield strength reduction factor R_y is required which will be determined from the modal pushover analysis of the structure. R_y is computed utilizing the following formula:

$$R_y = \frac{M^* \bar{A}}{V_{by}} \quad (3\text{-}8)$$

where $M^*$is the effective modal mass and V_{by} is the global yield strength under the modal pushover analysis. In Table 3-7, spectral acceleration values obtained from the target spectra, the corresponding target displacements and yield strength reduction factors are summarized.

Table 3-7 Spectral Acceleration, Target Displacements and Yield Strength Reduction Factors

	Model-C	**Transverse Period: 1.09 sec**		
	$\overline{\mathbf{A}}$ (g)	$\overline{\mathbf{D}}$ (m)	$\overline{\mathbf{D}}^{\mathbf{I}}$ (m)	**Ry**
OBE	0.506	0.149	0.150	0.9
MDE	1.090	0.322	0.333	1.9
MCE	1.706	0.504	0.547	3.0

	Model-B	**Transverse Period: 1.19 sec**		
	$\overline{\mathbf{A}}$ (g)	$\overline{\mathbf{D}}$ (m)	$\overline{\mathbf{D}}^{\mathbf{I}}$ (m)	**Ry**
OBE	0.444	0.156	0.156	0.8
MDE	0.998	0.351	0.360	1.8
MCE	1.563	0.550	0.583	2.8

In the implementation of modal pushover analysis, the pushover load quantity and distribution is determined as the multiplication of the mode shape (Φ) and the mass matrix (**M**). Through the inelastic modal pushover analysis, base shear-deck displacement curve of the structure is obtained. The yield strength (V_{by}) and the yield strength reduction factor are estimated after the idealization of the load-displacement curve. Pushover load is applied until one of the bridge columns reaches the ultimate curvature capacity.

Utilizing the Equations 3-9 and 3-10, the pushover curve is converted to the force-deformation (F_S/L - D) relation of an inelastic SDF system. Force-deformation curves of the SDOF systems for Model-B and Model-C are shown in Figure 3-8

$$F_s/L = \frac{V_b}{M^*} \qquad \textbf{(3-9)}$$

$$D = \frac{u_d}{\Gamma \varphi_d} \qquad \textbf{(3-10)}$$

in which L and Γ computed as ;

$$\boldsymbol{L = \Phi m l} \qquad \textbf{(3-11)}$$

$$\boldsymbol{\Gamma = (\Phi' m l)/(\Phi' m \Phi)} \qquad \textbf{(3-12)}$$

where V_b is the base shear under modal pushover, u_d is the deck displacement of the bridge under modal pushover analysis, Φ_d is the value of mode shape at the deck, Γ is the modal participation factor and l is the Influence vector

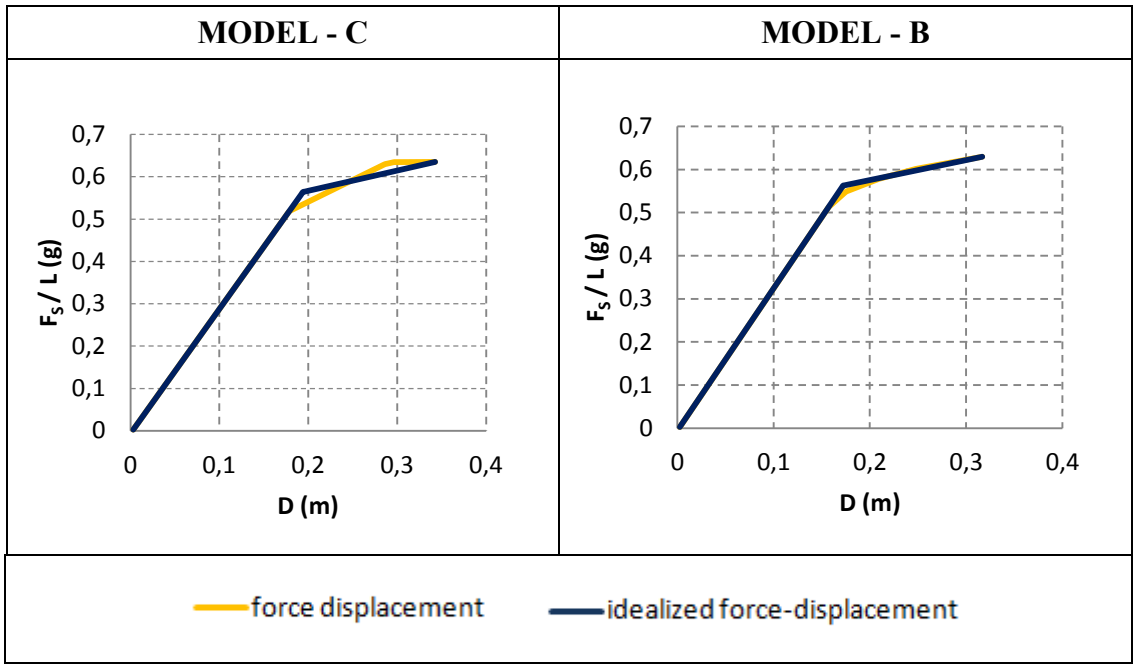

Figure 3-8 Idealized Pushover Curves for SDF System in Transverse Direction

The force deformation relationship (F_S/L-D) is used in the time history analysis of the inelastic SDOF system and the scale factor which causes the deformation sufficiently close to the target inelastic displacement is determined as the scale factor for the relevant earthquake record. The determination of the scale factor needs an iterative time history analysis of SDOF system. In this study, the SDOF systems are analyzed increasing the scale factors by 0.025 intervals at each iteration for each

ground motion. There can be more than one scale factor that satisfy the inelastic target displacement: the final scale factor is obtained as the minimum of the factors that yield a deformation within ±2% of the target inelastic deformation.

The scale factors for different target levels and bridge models are given in the Table 3-8 and Table 3-9. For the MPS procedure the scale factor for a given ground motion is determined independently of any other motions. However, for the ASCE method, the scale factors of the motions depend on the constituted motion sets. The second scale factor, i.e. SF_2, requires the consideration of the mean of the ground motion group, therefore, a given ground motion can have a different factor with regard to the group of motions it is used with.

The scale factors increase with the increase of target spectrum level as expected. For the Demirtas Viaduct, the lateral load capacity of the system, before the occurrence of plastic hinge in any of the columns is significantly high. Given the large target displacements for the MCE level, the scale factors for this target level reach very high values. Therefore, for this target level, an additional ground motion set is constituted selecting the motions with the lowest scale factors in the former ground motion sets, irrespective of the criteria of not using the same earthquake motion in a set. The scale factors obtained from the new set is given in Table 3-10

Table 3-8 Model C Scaling Factors

	MODEL C					
	OBE		MDE		MCE	
Motion	ASCE	MPS	ASCE	MPS	ASCE	MPS
1	0.849	0.35	1.553	0.875	2.435	1.45
2	2.901	2.75	7.249	5.95	11.344	9.525
3	1.448	0.775	2.722	1.725	4.268	4.375
4	1.268	0.7	2.943	2.125	4.609	3.675
5	1.016	0.525	1.874	1.05	2.939	1.475
6	1.020	0.525	1.873	1.05	2.937	1.75
7	0.606	0.5	1.425	1.075	2.231	1.975
8	0.633	0.25	1.445	0.9	2.263	1.375
9	0.580	0.45	1.309	1.675	2.050	2.4
10	0.562	0.425	1.062	1.025	1.665	2.85
11	0.587	0.525	1.369	1.2	2.143	2.925
12	2.486	2.075	4.690	4.425	7.355	5.9
13	1.942	1.1	3.701	3.05	5.804	5.45
14	2.329	1.325	5.549	3.325	8.688	6.85
15	0.696	0.3	1.623	0.9	2.542	1.75
16	1.594	1.325	3.586	2.775	5.615	4.125
17	5.157	5.35	12.372	13.4	19.369	22
18	0.792	0.525	1.793	1.05	2.809	1.475
19	0.538	0.625	1.267	1.3	1.983	2.275
20	3.794	3.975	9.473	10.475	14.828	16
21	0.476	0.375	1.158	1.25	1.813	2.525
22	1.414	1.55	3.260	2.975	5.103	7.025
23	1.294	1.1	3.038	2.3	4.756	5.575
24	1.230	0.65	2.930	1.9	4.587	3.225
25	1.368	1.525	3.381	3.275	5.294	4.95
26	0.589	0.375	1.309	1	2.050	1.45
27	0.764	0.65	1.739	1.2	2.724	2.125
28	1.491	1.375	3.459	3.3	5.416	4.5
29	1.299	0.825	2.978	2.375	4.664	3.225
30	1.292	0.625	2.897	2.425	4.536	5.225
31	0.700	0.55	1.700	1.175	2.662	2.375
32	1.333	0.925	3.006	1.925	4.706	4.9
33	1.352	1.225	3.164	2.6	4.953	3.925
34	2.690	2.475	6.186	5.175	9.684	8.625
35	1.434	1.125	3.341	3.025	5.230	5.475

Table 3-9 Model B Scaling Factors

	MODEL B					
	OBE		MDE		MCE	
Motion	ASCE	MPS	ASCE	MPS	ASCE	MPS
1	0.821	0.475	1.498	1.125	2.350	1.625
2	3.370	2.525	8.625	7.55	13.499	12.9
3	1.464	0.875	2.742	2.8	4.301	5.125
4	1.207	0.725	2.874	2.325	4.500	4.425
5	0.994	0.575	1.830	1.125	2.871	1.65
6	1.003	0.55	1.848	1.275	2.899	2.475
7	0.618	0.55	1.495	1.125	2.341	2.3
8	0.635	0.3	1.475	1.1	2.309	1.625
9	0.575	0.45	1.307	1.85	2.047	2.55
10	0.580	0.4	1.104	1.15	1.731	3.25
11	0.571	0.625	1.363	1.475	2.134	3.175
12	2.510	1.875	4.721	3.675	7.404	6.175
13	1.984	1.325	3.772	4.025	5.915	6.2
14	2.324	1.475	5.674	3.925	8.884	7.3
15	0.685	0.3	1.607	1.25	2.517	2.1
16	1.567	1.925	3.547	3.975	5.554	5.75
17	5.289	5.925	12.991	12.7	20.339	21.775
18	0.745	0.55	1.730	1.075	2.709	1.775
19	0.548	0.575	1.292	1.475	2.023	2.425
20	4.213	4.75	10.584	13.225	16.568	16.975
21	0.494	0.375	1.214	1.4	1.900	3.175
22	1.407	1.8	3.252	3.75	5.091	7.25
23	1.320	1.3	3.098	2.7	4.850	6.575
24	1.242	0.55	2.986	2.125	4.676	3.9
25	1.438	1.65	3.558	4	5.570	5.65
26	0.587	0.425	1.318	1.15	2.063	1.65
27	0.734	0.825	1.670	1.85	2.615	2.325
28	1.463	1.875	3.388	3.975	5.305	5.1
29	1.266	1	2.905	2.7	4.550	3.675
30	1.301	0.85	2.964	3.225	4.641	6.325
31	0.735	0.675	1.800	1.8	2.817	2.5
32	1.317	1.05	2.993	2.675	4.686	5.35
33	1.401	1.45	3.282	3.25	5.138	7.575
34	2.799	2.325	6.486	5.575	10.155	10.8
35	1.450	0.8	3.373	3.6	5.282	5.75

Table 3-10 ASCE Scale Factors for Set-6 for DLH (D3) Spectrum

MODEL C

	Scale Factors		
Motion	**New Set**	**Previous Set**	**Previous Motion Set**
7	2.496	2.231	2
9	2.382	2.050	4
10	1.799	1.665	1
11	2.397	2.143	2
19	2.288	1.983	5
21	1.881	1.813	3
26	2.382	2.050	4

MODEL B

	Scale Factors		
Motion	**New Set**	**Previous Set**	**Previous Motion Set**
7	2.553	2.341	2
9	2.349	2.047	4
10	1.804	1.731	1
11	2.327	2.134	2
19	2.309	2.023	5
21	1.910	1.900	3
26	2.368	2.063	4

CHAPTER 4

EVALUATION OF THE ANALYSIS RESULTS

The two inelastic models, B and C, are analyzed with the scaled and unscaled motions and the results are presented in this chapter. A total of 245 analyses are conducted for one of the models, using the two scaling procedures at three different demand levels. A total of 490 analyses are carried out for both of the analyzed systems. The analyses results are interpreted in terms of drift ratios or displacements at the superstructure level given these are the common parameters for evaluating the demand/capacity levels for bridge systems. It should be noted that the results provided here does not form an assessment of the Demirtas Viaduct behavior and should not be interpreted as such.

4.1 ANALYSIS RESULTS

In contrast to the common analysis approach for structures based on response spectrum loading, the use of time history methods poses an additional difficulty. Given a design/assessment problem, different engineers may reach completely different results just based on the ground motions selected for the evaluation, irrespective of the tools utilized in the analyses. Even if it is assumed that the computational resources available to the engineer, the software capabilities and the experience/knowledge of the engineer are ideally provided, the variability in the selection of ground motions can still lead to very significant conclusions on the same design/assessment issue. The scaling methods are based on this premise and are used to reduce the variability in the assessment results to reach sound, dependable engineering results. The results of the scaling, in this context, are evaluated in terms of accuracy, efficiency and consistency of the results from the selected sets.

The goal of any selection procedure is to obtain time history results close to the expected behavior of the system with low amount of variability and a minimal effort. The accuracy of the analysis results are implied by the closeness of the mean of the EDP values to the expected response, which is usually defined a benchmark value for the target spectrum. Accuracy is estimated as the ratio of the mean of the sets to the benchmark value (Equation 4-1). The closeness of that ratio to the unity shows to what extent the scaling method predicts the "true" demands.

The “true” demand for a structural system is the expected value of the EDP for the range of possible motions that can be experienced at the site. It is hard to quantify as expected, given the level of ground motion data as well as the simulation of motions at a site is not at an adequate stage to form a complete picture of the demand at the site. Therefore, response spectra based quantities are often used to estimate mean demand levels, in terms of displacements and accelerations, as these design spectra are based on a large number of ground motions obtained from sites with similar properties and similar fault conditions. The expected demand will be referred as the “true” demand in the rest of the work for the sake of brevity.

In this study, for OBE target level, the benchmark value is determined as the geometric mean of the displacement values obtained from the 35 unscaled motions while for MDE and MCE target levels, the benchmark values are estimated using spectral displacements. The inelastic displacement target, i.e. the benchmark displacements for MDE and MCE cases, is obtained using the corresponding spectra (along with Equation 3-6, the C_R modification factor). Benchmark drift values are estimated as the division of the benchmark displacements to the height of the nodes for which the demand parameter is required. The benchmark displacements and drifts are summarized in Table 4-1.

Benchmark displacements for MCE level appears to be greater than the displacement capacity which has been obtained as 39 cm from moment-curvature equations. However, this is not taken into the consideration as capacity-demand evaluation is not considered in this study.

Table 4-1 Benchmark Displacements and Drifts

	Benchmark Displacement (cm)		Benchmark Drift (%)	
	B	**C**	**B**	**C**
OBE	15.3	15.4	0.55	0.54
MDE	35.9	33.3	1.24	1.17
MCE	58.2	54.6	2.01	1.92

The accuracy of the estimate for any set of ground motion analysis is then evaluated based on the following measure. The mean EDP of the set, divided by the benchmark target provides a measure of how well the used ground motion records in reaching the intended target demand.

$$accuracy = \frac{mean\ EDP\ of\ sets}{benchmark\ EDP} \quad (4\text{-}1)$$

Dispersion measure is the second criterion for the evaluation and comparison of the scaling methods. Computed within a set, the measure is an intra-set indicator of variability of the results. If the variance of the computed EDP values within a given set is small, then the method is considered as efficient indicating that the smaller number of records is needed to predict the "true" demand for a determined confidence level (Kalkan et al., 2012). The coefficient of variation (COV) of the EDP values in a given set is used for the estimation of the dispersion measure. A large value for a dispersion value would indicate large variability of results within the test and show that the results of the models should be interpreted carefully as they are sensitive to modeling and/or time history input.

Consistency is the measure for the variability of mean values obtained from the scaled sets. Computed among the mean values of the ground motion sets, the measure is an inter-set indicator of the variability of the results. The coefficient of variation among the mean EDP values of different sets is computed. In other words, consistency is the variability of 5 mean values for 5 sets. A large value for a dispersion value would indicate large variability among the results of possible ground motion set. Such a result would mean problems in efficiency as well as the accuracy of the chosen approach. Results of the models should be interpreted

carefully as they are sensitive to modeling and/or time history input. Consistency is also an important criterion because variations in the results for different motion sets would make the scaling procedure unreliable.

In this study, maximum drift values are used for the comparison of the results. The point which has the maximum value in the eigenvector for the transverse mode is considered as the EDP location. The maximum displacement point is at the middle of the deck on the third span for Model C and at the top of the Pier-10 for Model B. The maximum drifts for the OBE demand level are shown in Figure 4-1 and Figure 4-2 respectively, for models C and B. The maximum drifts for the MDE demand level are shown in Figure 4-3 and Figure 4-4 respectively, for model C and B. Finally, the maximum drifts for the MCE demand level are shown in Figure 4-5 and Figure 4-6, respectively, for model C and B. In these figures, the drift levels are provided first for a ground motion set including all ground motions. Then, for the chosen 5 sets, the drift levels are provided and compared to the benchmark levels.

The (COV) value is calculated for 35 scaled and unscaled motions to see the variability of the results without scaling and given in the Table B-1 and Table B-2 in Appendix B. Maximum drift values obtained from scaled motions for MDE and MCE target levels for both models are provided in Table B-3 and B-4 in Appendix B. In addition, the (COV) values for the sets are estimated since the scale factors for ASCE changes according to the ground motions in the sets.

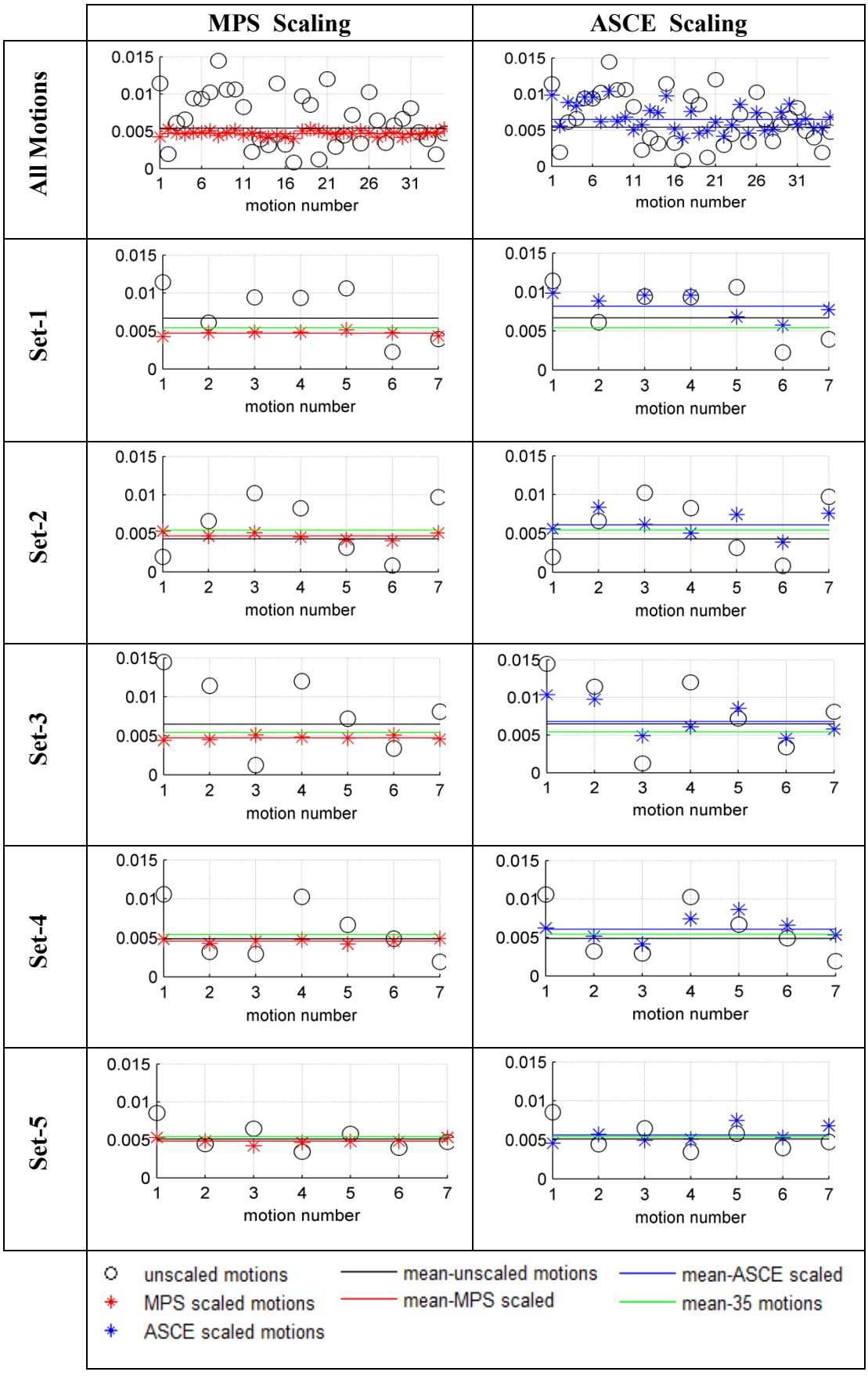

Figure 4-1 Model C OBE - Maximum Drift

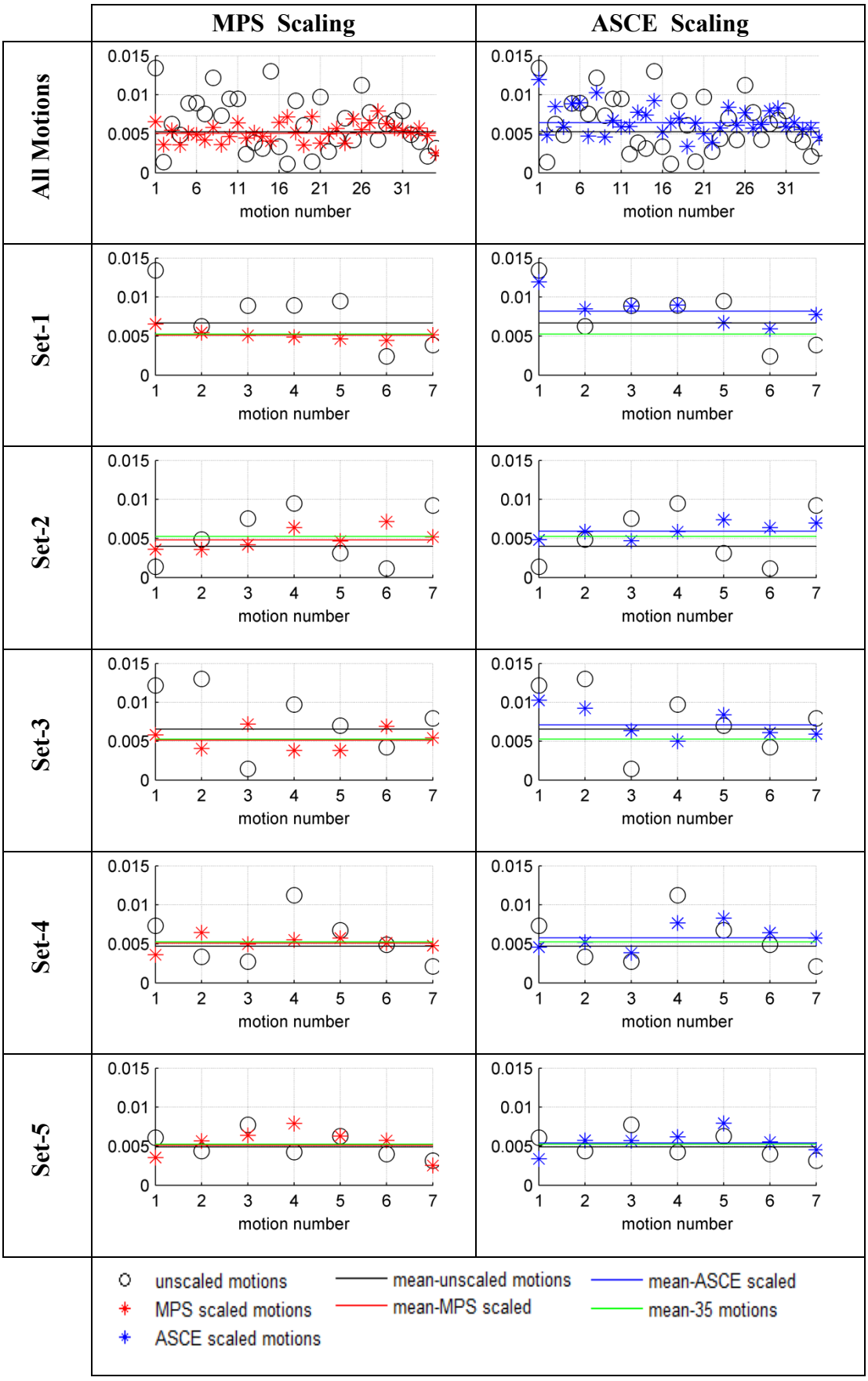

Figure 4-2 Model B OBE - Maximum Drift

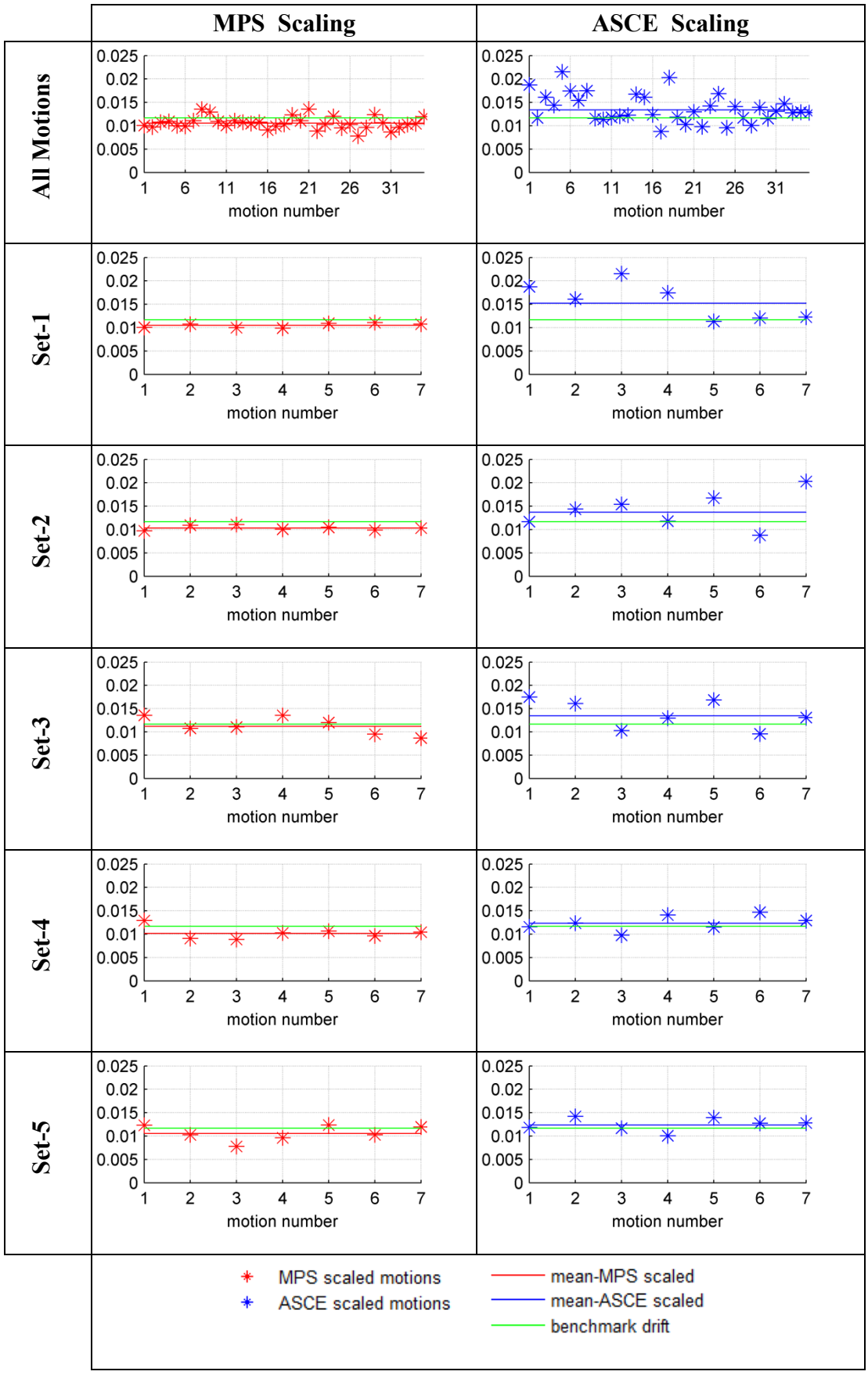

Figure 4-3 Model C MDE - Maximum Drift

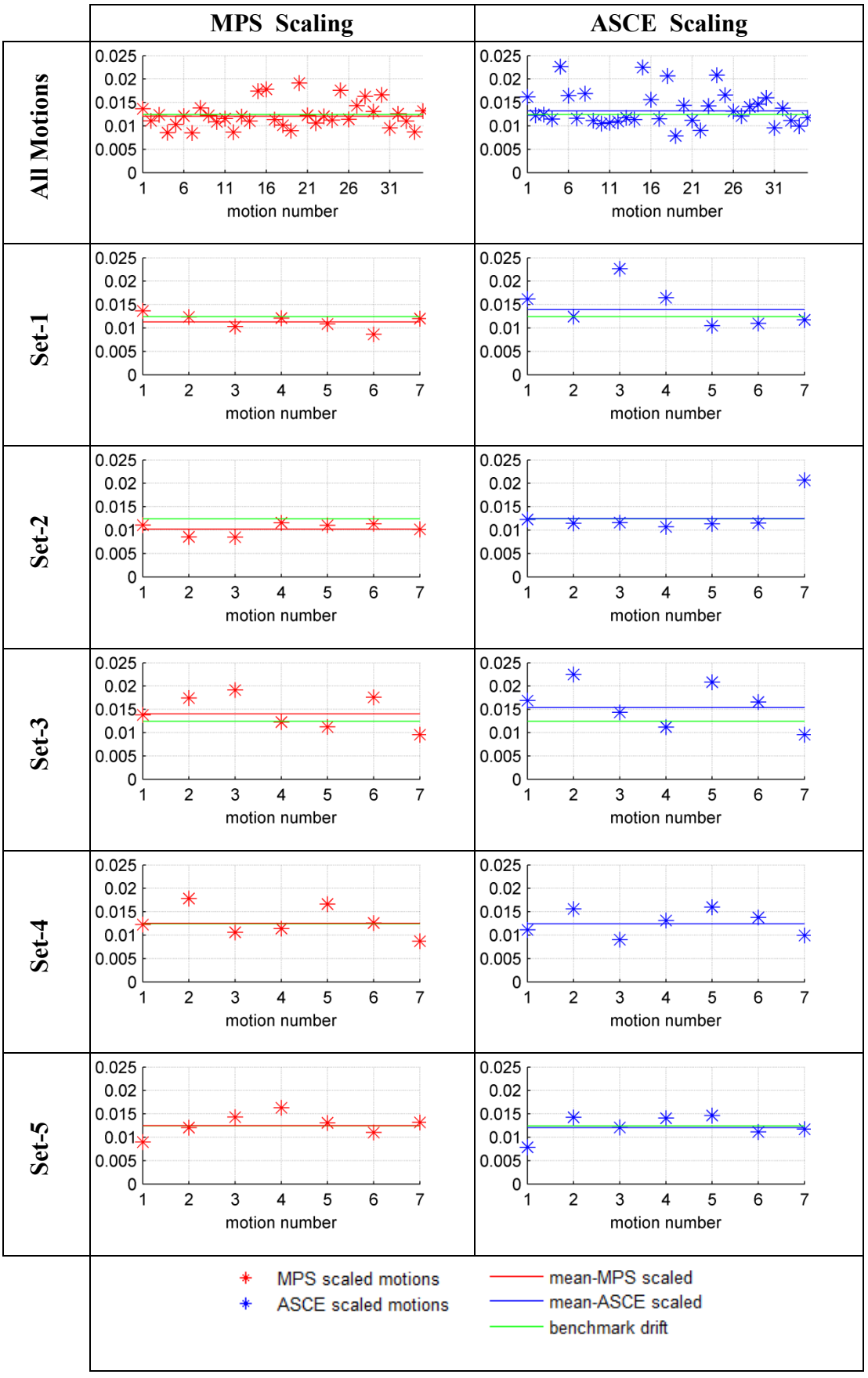

Figure 4-4 Model B MDE- Maximum Drift

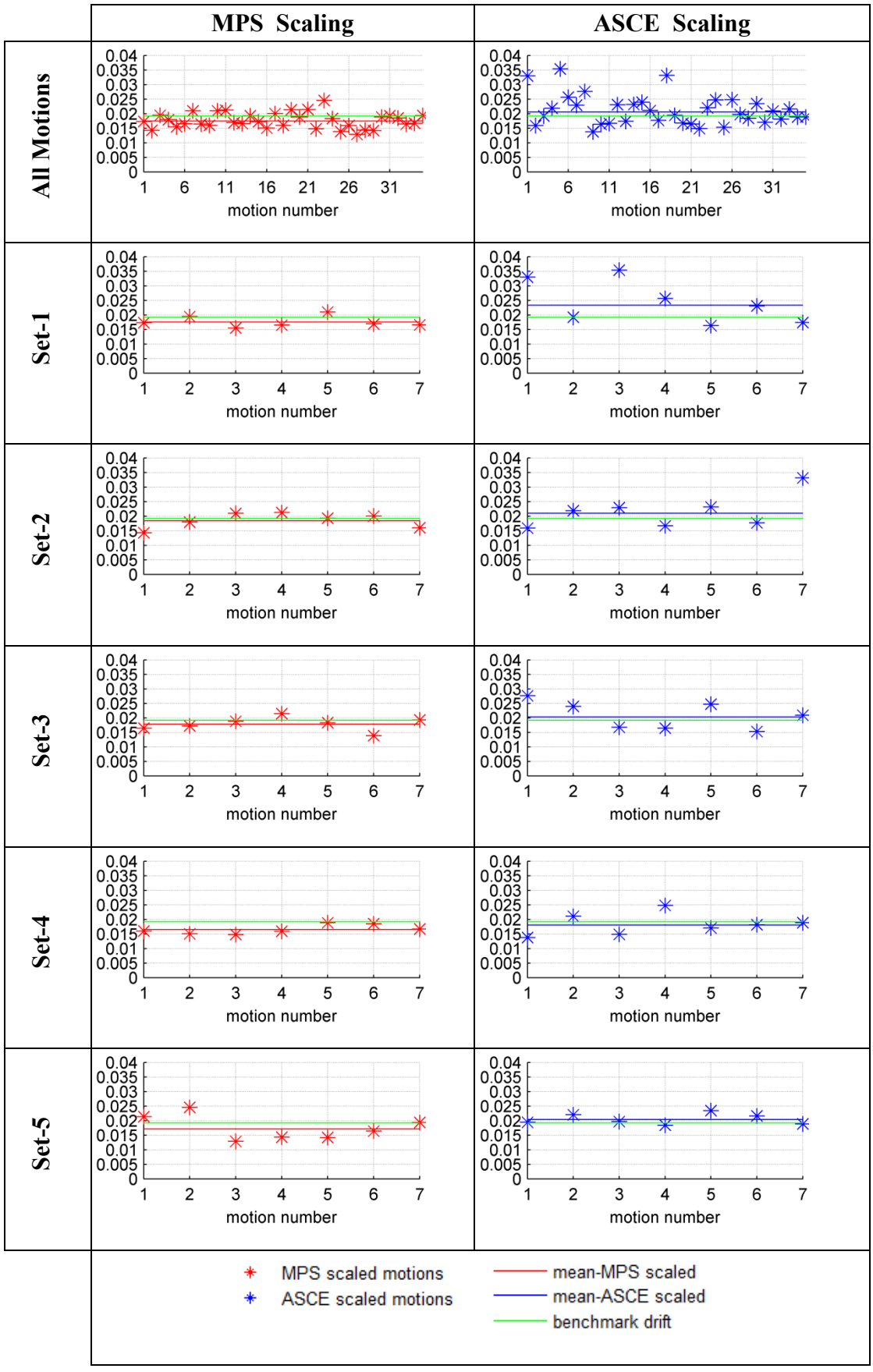

Figure 4-5 Model C MCE - Maximum Drift

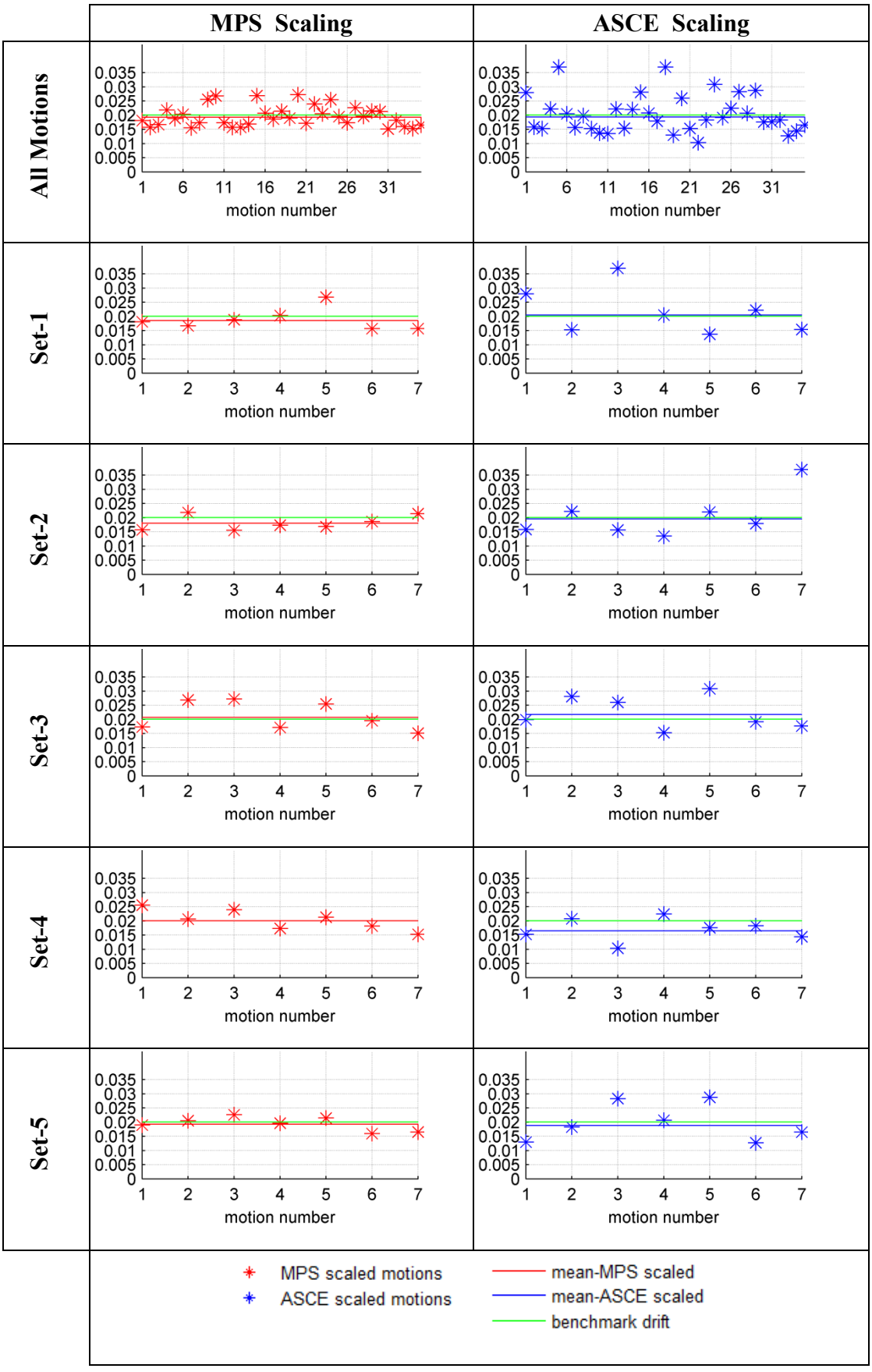

Figure 4-6 Model B MCE - Maximum Drift

4.2 EVALUATION OF RESULTS

As indicated before, the scaling methods can be evaluated in terms of accuracy (similarity to the benchmark demands), efficiency (intra-set variance) and consistency (inter-set variance). In order to see the results clearly, the ratio of the mean values to the goal drift values and the (COV) values for all sets are presented in Figure 4-7 and Figure 4-8.

Considering mean estimates of EDPs, the following conclusions can be drawn from the results;

- MPS procedure underestimates the mean values of the sets when compared to the benchmark values for almost all cases while the opposite is true for the ASCE scaling procedure. With ASCE scaling, the benchmark value is underestimated for 7 cases out of 32, while for MPS, the benchmark value is overestimated for only 5 cases out of 32.
- The largest discrepancy of the mean results of a set with respect to the benchmark results is obtained as 18% for the MPS technique. As much as 55% discrepancy is obtained for the ASCE scaling. The mean results from the ASCE estimation are considerably different than the target levels for some cases.
- With the increasing target level, the accuracy of the MPS estimates does not seem to change. However, the estimates for ASCE scaling get closer to the target level for both models B and C in an obvious manner. The effect of the target level is clearly observed on the ASCE estimates. The reason for this behavior is thought to be the equal displacement rule, in the sense that the higher scaling of the motions above the yield levels basically push all displacements towards the same target quantity. For the lower target levels, some motions are observed in the elastic range and the displacement content would be affected significantly by the shape of the spectra.

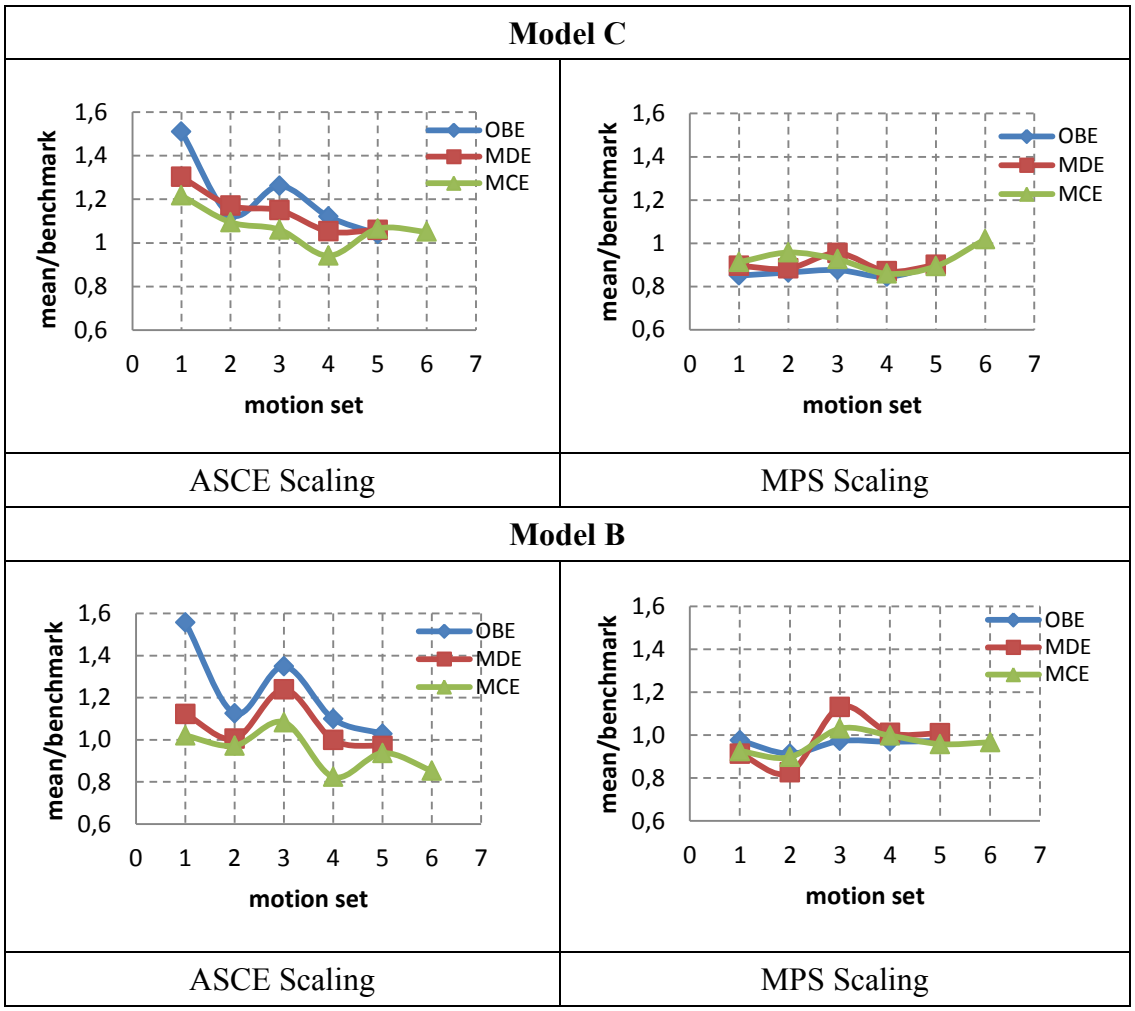

Figure 4-7 Accuracy of the Estimates, Mean EDP vs. Benchmark

The dispersion within the selected sets are presented in Figure 4-8

- Without the scaling of motions, (i.e. using all the 35 motions as a single set), the dispersion of the demand parameter is very large. A coefficient of variation of 0.60-0.70 is obtained (Table B-1 and Table B-2). The record to record variability of the drift values decreases considerab1y if scaling is applied to the motions,
- The dispersion of the drift values due to the scaled motions is greater for the larger model, model B. This is an expected result given the more complex nature of this model and additional interactions between the spans through the expansion joints. This trend is valid for both scaling techniques. The dispersion reduces considerably for model C.

- The dispersion in the results is considerably smaller for the MPS technique compared to the ASCE scaling. This trend is valid for both models as well.
- There appears to be no correlation between the target level and the dispersion within the data set. (Figure 4-8).
- Consistency between the mean values of the MPS scaled sets decreases in small quantities (target-1:0.0238, target-2:0.0357, target-3:0.0596), with the increase of target spectrum while such a trend is not followed by the larger model.

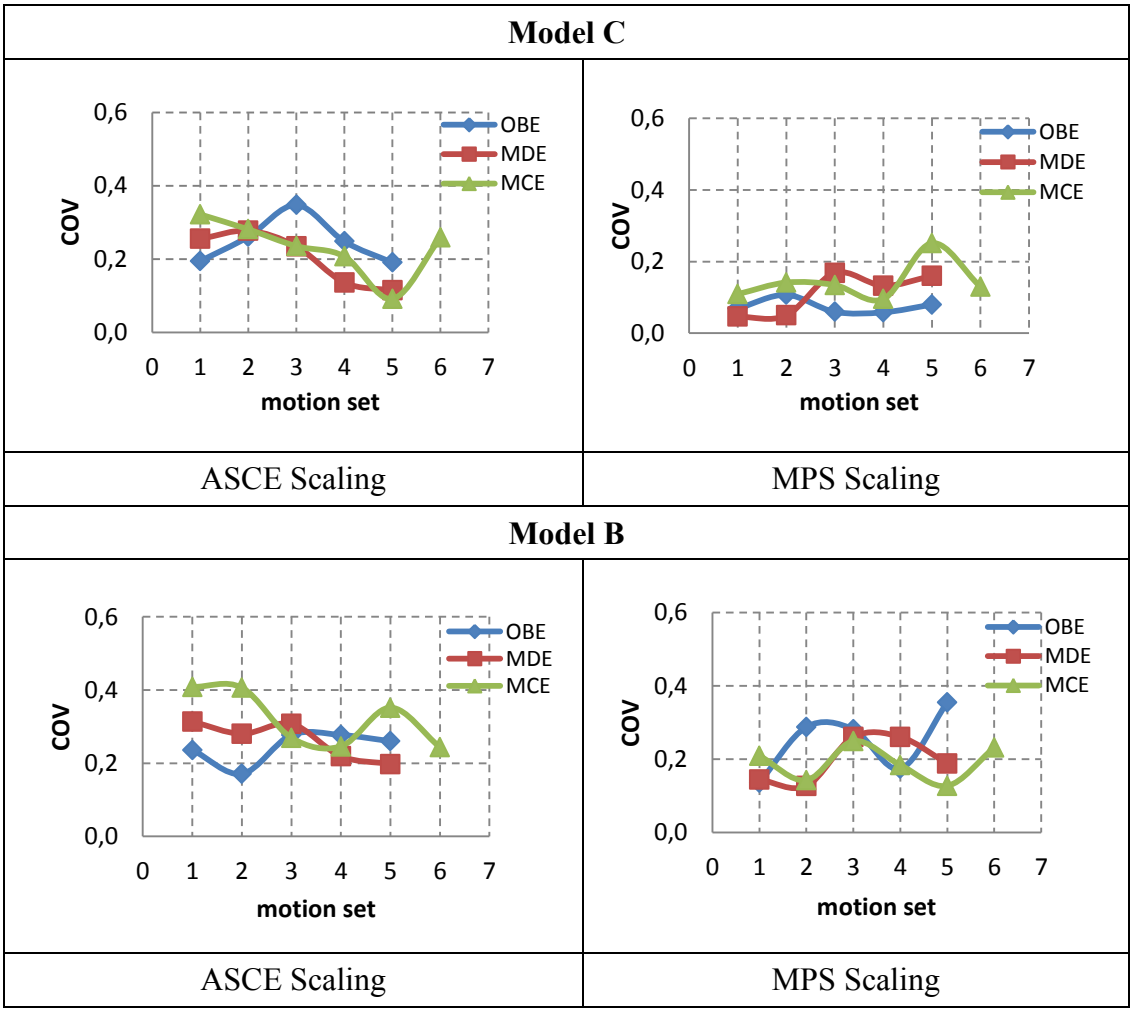

Figure 4-8 Efficiency of the Estimates

The consistency among the sets is an indicator of the efficiency of the model as well as the accuracy of the approach. The consistency of the results, as indicated by the

coefficient of variation among the mean estimates of each set for each target level is presented in Table 4-2 and Figure 4-9 for models B and C. Excluding the case of MDE target spectrum, the variation between the mean of the sets is smaller for MPS when compared to ASCE procedure indicating MPS gives more consistent results. The reduction in coefficient of variation for the ASCE scaling with increasing target demand is also evident. For MPS scaling, no such trend is observed.

Table 4-2 Coefficient of Variation of the Mean Values

	MODEL B		MODEL C	
	ASCE	**MPS**	**ASCE**	**MPS**
OBE	0.179	0.028	0.153	0.024
MDE	0.106	0.118	0.089	0.036
MCE	0.105	0.050	0.083	0.060

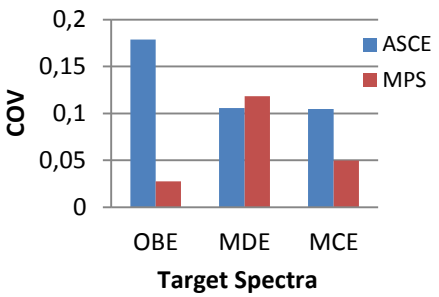

Model B

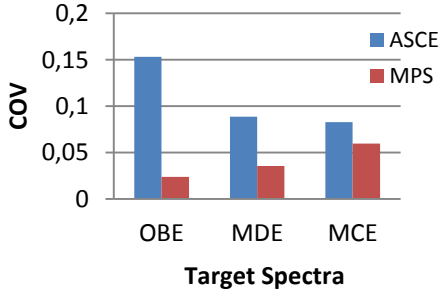

Model C

Figure 4-9 Consistency of Estimates, Coefficients of Variation of the Estimates Inter-Set

CHAPTER 5

CONCLUSION AND OUTLOOK

5.1 CONCLUSION

In this study the use of two scaling procedures namely the modal pushover based scaling (MPS) and ASCE/SEI Standard (2010) procedure is compared for two different analytical models of a pre-tensioned bridge for different seismic demand levels. 35 ground motion records are selected to this end, based on the magnitude of the event, distance to the fault and the $V_{s,30}$ value at the bridge site. Target parameters necessary for scaling are determined from three different target spectra including geometric mean of the 35 unscaled motions, AASHTO (2010) design spectrum for the events with 1000-year return period and finally DLH design spectrum for the events with 2475-year return period which correspond to operation based event (OBE), maximum design event (MDE) and maximum considered event (MCE), respectively. Two bridge models of the Demirtas Viaduct differing from each other in terms of their span numbers are used in order to investigate the variability in the response of the system due to the analytical modeling approach. The scale factors for ASCE and MPS procedures are determined for each target spectrum.

The ASCE scaling approach includes a second factoring coefficient requiring the use of new factors for every ground motion depending on the suite it is placed in. Therefore, 5 randomly chosen ground motion sets of 7 motions are constituted to compare the scaling procedures. The scaling factor for the MPS procedure is unique for a given motion and are independently determined regardless of the set for which the motion is at. Scaling the motions, the critical EDP for the bridge system, i.e. the drift ratio at the critical bents, are compared with each other for the two scaling procedures, target earthquake levels and the different bridge models.

Main findings & conclusions of the study can be summarized as follows:

- Both of the scaling procedures decrease the variability of drift values when compared to the dispersion obtained from the analyses carried out with unscaled motions.
- The dispersion of MPS scaled sets is smaller than that of ASCE scaled sets in most of the cases since MPS method defines scaling factors according to a target displacement considering structural capacity. Correspondingly, mean values of the sets are more consistent almost for all cases when the motions are scaled by MPS procedure.
- Although the mean values obtained by ASCE scaled motions are close to the benchmark values, the counter values obtained by MPS procedure are in the range of ±20% difference from the benchmark for all cases. The MPS procedure can be considered more reliable in terms of forecasting the drift demands in a certain range from the "true" mean.
- The accuracy of mean values seems to be affected by the determined target spectrum for ASCE scaling procedure while there is small influence of target spectrum on the mean values for MPS procedure. The coefficient of variation for the predicted drift ratio reduced for ASCE scaling for higher demand levels indicating the possible use of less motions or less sensitivity to the suite selection for higher seismic demand levels
- The complexity of the analytical model increases the variability obtained from each scaling procedure. However, the inter-set variation for MPS, even for the more complex model, appears to be on par or lower than the inter-set variation obtained for ASCE scaling for the simpler analytical model.
- Given the Demirtas Viaduct represents a typical sample for overpasses with less than 30 m pier heights, the results can be applied to a large range of highway bridges in Turkey subject to high seismic hazard.

5.2 OUTLOOK

Based on the findings of this thesis, potential future studies can be stated as follows;

- The scaling procedures are applied to the two bridge models considering transverse direction in this study. However the natural vibration periods in transverse direction of the two bridges are obtained very close to each other. The scaling could be extended to different structural idealizations of the same system, such as the full bridge model, in order to investigate the effect of the complexity of the model on the results.
- More ground motion sets can be used with the ASCE scaling procedure in order to obtain the statistical confidence intervals of the results provided by ASCE scaling.
- The use of multi-direction ground motion and the corresponding scaling for the vertical and horizontal components together should be studied.
- The bridge models can be improved in order to include the effect of bearing nonlinearity on the response.
- In addition to the drift values, different engineering demand parameters can be compared.
- Multiple support excitation and its effects on the scaling of the ground motions for such long bridges can be investigated.
- This study has been conducted for high seismic hazard with M_w values between 6.5-7.9 and 0-12 km fault distance. Moderate intensity events would lead to different ground motion sets the effect of which can be investigated.

REFERENCES

1. AASHTO - American Association of State Highway and Transportation Officials (2010). LRFD Bridge Design Specifications, Customary U.S. Units Washington DC.
2. AASHTO - American Association of State Highway and Transportation Officials (2011). LRFD Seismic Bridge Design, Customary U.S. Units Washington DC.
3. AASHTO - American Association of State Highway and Transportation Officials (2012). LRFD Bridge Design Specifications, Customary U.S. Units Washington DC.
4. Abrahamson, N.A. and Silva, W.J. (1997). Empirical response spectral attenuation relations for shallow crustal earthquakes, Seismological Research Letters, Vol. 68, pp. 94-127.
5. ASCE - American Society of Civil Engineers (2010). Minimum Design Loads for Buildings and Other Structures, ASCE/SEI 7-10.
6. DLH (2007). Kıyı ve Liman Yapıları, Demiryolları, Havameydanları İnşaatları Deprem Teknik Yönetmeliği.
7. Aviram, A., Mackie, K.R. and Stojadinović, B. (2008). Guidelines for nonlinear analysis of bridge structures in California. Pacific Earthquake Engineering Research Center.
8. Baker, J.W. and Cornell, C.A. (2006). Which spectral acceleration are you using. Earthquake Spectra, Vol. 22, pp. 293–312.
9. Bazzurro, P. (1998). Probabilistic Seismic Demand Analysis, Ph.D. Thesis, Department of Civil and Environmental Engineering, Stanford University, California.
10. Bommer, J.J., Scott, S.G. and Sarma, S.K. (2000a). Hazard-consistent earthquake scenarios. Soil Dynamics and Earthquake Engineering, Vol. 19, pp. 219–231.
11. Bommer, J.J. and Scott S.G. (2000b). The feasibility of using real accelerograms for seismic design, Implications of recent earthquakes on seismic risk, pp. 115-126, Imperial College Press, London.
12. Bommer, J.J. and Acevedo, A.B. (2004). The use of real earthquake accelerograms as input to dynamic analysis, Journal of Earthquake Engineering, Vol. 8, pp. 43-91.
13. CALTRANS - California Department of Transportation (2006). Seismic Design Criteria (SDC), Version 1.4, Sacramento, California.
14. CALTRANS - California Department of Transportation (2013). Seismic Design Criteria (SDC), Version 1.7, Sacramento, California.

15. Chopra, A. and Chintapakdee, C. (2004). Seismic response of vertically irregular frames: response history and modal pushover analyses. Journal of Structural Engineering, Vol. 130:8, pp. 1177-1185.

16. Cordova, P.P., Deierlein, G.G., Mehanny, S.S.F. and Cornell, C.A. (2000) Development of a two-parameter seismic intensity measure and probabilistic assessment procedure, Proceedings of the 2nd U.S.-Japan Workshop on Performance-Based Seismic Design Methodology for Reinforced Concrete Building Structures, Pacific Earthquake Engineering Research Center, University of California, Berkeley, CA.

17. Duygu M. B. (2014). Ground motion scaling for the prediction of the seismic response of concrete gravity dams, Master Thesis, Department of Civil Engineering, METU, Ankara.

18. Eurocode 8 (2005). Design of structures for earthquake resistance-Part 2: Bridges, Final Draft prEN 1998-2, European Committee for Standardization, Brussels, Belgium.

19. Goel, R.K. and Chopra, A.K. (2008). Estimating seismic demands for 'ordinary' bridges crossing fault-rupture zones, Report no. UCB/ EERC-2008/01, Earthquake Engineering Research Center, University of California, Berkeley.

20. Graizer V. and Kalkan, E. (2009). Prediction of Response Spectral Acceleration Ordinates based on PGA Attenuation, Earthquake Spectra, Vol.25:1, pp. 36–69.

21. Hancock J., Watson-Lamprey J, Abrahamson N, Bommer J.J., Markatis A, McCoy E and Mendis R. (2006). An improved method of matching response spectra of recorded earthquake ground motion using wavelets, Journal of Earthquake Engineering Vol.10:1, pp. 67–89.

22. Hancock J. and Bommer J.J. (2007). Using matched records to explore the influence of strong-motion duration on inelastic structural response, Soil Dynamics and Earthquake Engineering, Vol. 27, pp. 291–299.

23. Heo, Y., Kunnath, S.K. and Abrahamson, N. (2011). Amplitude-Scaled versus Spectrum-Matched Ground Motions for Seismic Performance Assesment, Journal of Structural Engineering, Vol.137, pp. 278-288.

24. Kalkan, E. and Chopra, A. (2010). Practical Guidelines to Select and Scale Earthquake Records for Nonlinear Response History Analysis of Structures, US Geological Survey Open-File Report, 2010, 1068.2010: 126.

25. Kalkan, E. and Kunnath, S.K. (2006). Effects of fling-step and forward directivity on the seismic response of buildings, Earthquake Spectra, Vol. 22:2, pp. 367–390.

26. Katsanos, E.I., Sextos, A.G. and Manolis, G.D. (2010). Selection of earthquake ground motion records: A state-of-the-art review from a structural engineering perspective, Soil Dynamics and Earthquake Engineering, Vol. 30:4, pp. 157–169.

27. Kawashima, K., (2000). Seismic design and retrofit of bridges, Proceedings of The Twelfth World Conference on Earthquake Engineering, Auckland, New Zealand.

28. Kurama, Y. and Farrow, K. (2003). Ground motion scaling methods for different site conditions and structure characteristics, Earthquake Engineering and Structural Dynamics, Vol. 32, pp. 2425-2450.

29. Lilhanand, K. and Tseng, W.S. (1988). Development and application of realistic earthquake time histories compatible with multiple-damping design spectra, Ninth World Conference on Earthquake Engineering, Vol. 2, pp. 7-8.

30. Luco, N. and Cornell, A.C. (2007). Structure-specific scalar intensity measures for near-source and ordinary earthquake ground motions, Earthquake Spectra, Vol. 23:2, pp. 357–392

31. Mander, J.B., Priestley, M.J.N. and Park, R. (1988). Theoretical stress-strain model for confined concrete, Journal of the Structural Engineering, Vol. 114:8, pp. 1804–1826.

32. Mazzoni, S., McKenna, F., Scott, M.H. and Fenves, G.L (2006). OpenSees Command Language Manual, Open System for Earthquake Engineering Simulation (OpenSees).

33. Mehanny, S. (1999). Modeling and assessment of seismic performance of composite frames with reinforced concrete columns and steel beams, Ph.D. Thesis, Department of Civil and Environmental Engineering, Stanford University, California.

34. Mestav, G. (2014). Comparison of mean site-specific response spectra in turkey with the design spectra of AASHTO LRFD bridge design specifications (2007 and 2010), Master Thesis, Department of Civil Engineering, METU, Ankara.

35. Naeim, F. and Lew, M. (1995). On the use of design spectrum compatible time histories. Earthquake Spectra, Vol.11:1, pp. 111-127.

36. O'Donnell, A.P., Beltsar, O.A., Kurama, Y.C., Kalkan, E. and Taflanidis, A.A. (2011). Evaluation of ground motion scaling methods for analysis of structural systems. ASCE Structures Congress.

37. O'Donnell, A., Kurama, Y., Kalkan, E. and Taflanidis, A. (2013). Experimental evaluation of ground motion scaling methods for nonlinear analysis of structural systems. ASCE Structures Congress, Bridging Your Passion with Your Profession, pp. 2180-2191.

38. OpenSees. (2009). Open Source finite element platform for earthquake engineering simulations. Pacific Earthquake Engineering Center, University of California, Berkeley, CA.

39. PEER (2013). PEER NGA database. [Online] Available at: http://ngawest2.berkeley.edu/ [Accessed 12 February 2015].

40. Priestly, M.J.N. and Calvi, G.M. (1996). Seismic Design and Retrofit of Bridges, John Wiley & Sons, Inc., USA.

41. Reyes, J.C. and Kalkan, E. (2012). How many records should be used in an ASCE/SEI-7 ground motion scaling procedure? , Earthquake Spectra, Vol. 28, pp. 1223-1242.

42. Reyes, J.C., Riaño, A.C., Kalkan, E., Quintero, O.A. and Arango, C.M. (2014). Assessment of spectrum matching procedure for nonlinear analysis of symmetric- and asymmetric-plan buildings, Engineering Structures, Vol. 72 , pp. 171-181.

43. SAP 2000 (2011) v.15.0.0, Computers and Structures Inc., Berkeley, CA.

44. Sevgili, G. (2007). Seismic performance of multisimple-span skew bridges retrofitted with link slabs, Master Thesis, Department of Civil Engineering, METU, Ankara.

45. Shome, N., Cornell, C.A., Bazzurro, P. and Carballo, J.E. (1998). Earthquakes, records and nonlinear responses, Earthquake Spectra, Vol. 14, pp. 469-500.

46. Shome, N. and Cornell, C. (1999). Probabilistic seismic demand analysis of nonlinear structures, Reliability of Marine Structures Program Report No. RMS-35, Department of Civil and Environmental Engineering, Stanford University.

47. Tothong, P., and Cornell, A.C. (2008). Structural performance assessment under near-source pulse-like ground motions using advanced ground motion intensity measures. Earthquake Engineering and Structural Dynamics, Vol. 37:7, pp.1013–1037

48. TÜBİTAK KAMAG 110G093, (2015) Türkiye Köprü Mühendisliğinde Tasarım ve Yapıma İlişkin Teknolojilerin Geliştirilmesi Teknik Klavuzu, pp. 582-586; pp. 767-768.

49. UCFYBER-Cross Section Analysis Structural Software (1999), Chadwell C.B., Department of Civil and Environmental Engineering, University of California, Berkeley, CA.

50. Watson-Lamprey, J. and Abrahamson, N. (2006). Selection of ground motion time series and limits on scaling, Soil Dynamics and Earthquake Engineering, Vol. 26, pp. 477-482.

APPENDIX A

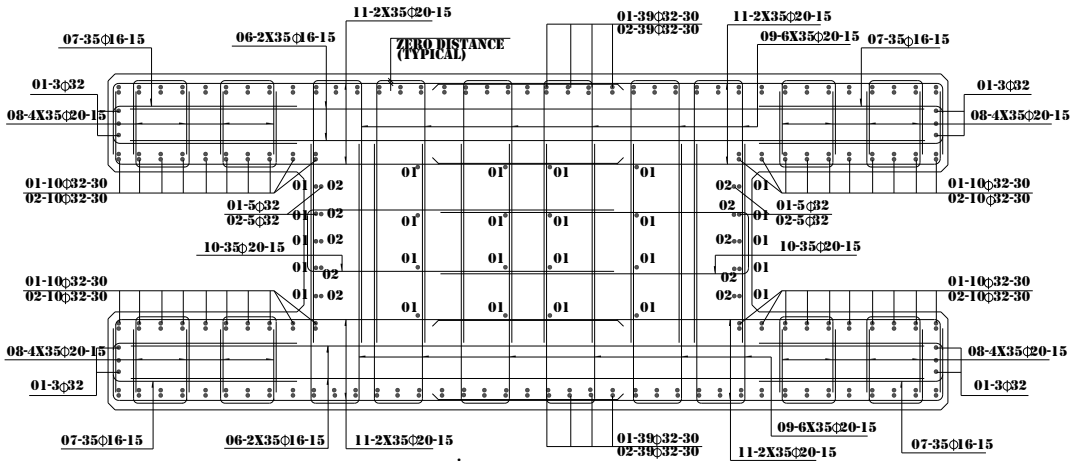

Figure A- 1 Bottom Cross-Section of Pier-10

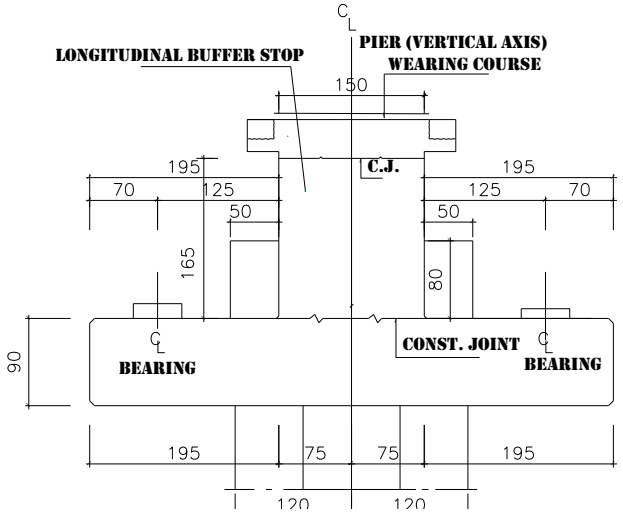

Figure A- 2 Typical Column Top without Expansion Joint

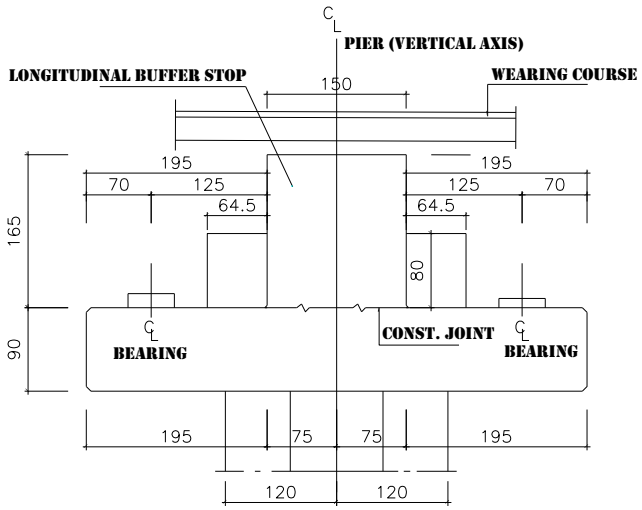

Figure A- 3 Typical Column Top with Expansion Joint

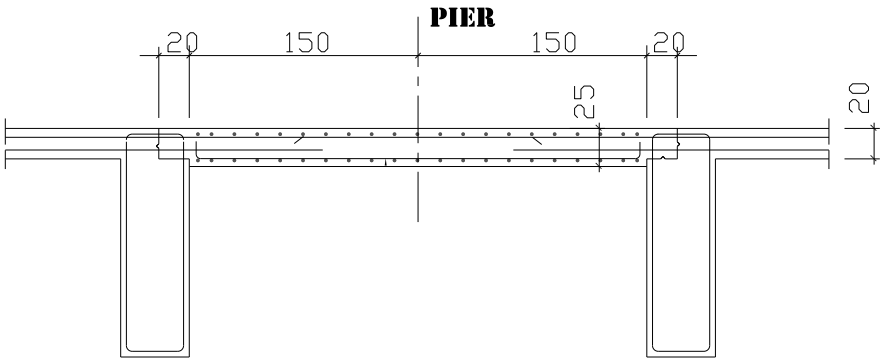

Figure A- 4 Deck Elevation View at Pier

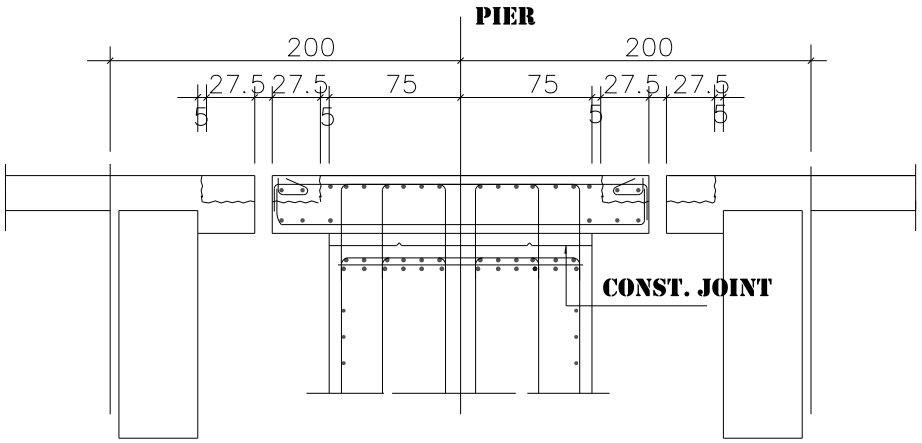

Figure A- 5 Deck Elevation View at Pier Expansion Joint

APPENDIX B

Table B - 1 Maximum Drift for Model B -OBE

Motion #	Unscaled	ASCE	MPS
1	0.0139	0.0124	0.0068
2	0.0014	0.0050	0.0037
3	0.0065	0.0088	0.0056
4	0.0051	0.0061	0.0037
5	0.0092	0.0092	0.0053
6	0.0093	0.0093	0.0050
7	0.0078	0.0049	0.0043
8	0.0126	0.0106	0.0060
9	0.0076	0.0047	0.0037
10	0.0098	0.0070	0.0048
11	0.0098	0.0061	0.0066
12	0.0025	0.0061	0.0046
13	0.0040	0.0080	0.0053
14	0.0032	0.0077	0.0048
15	0.0135	0.0096	0.0042
16	0.0035	0.0054	0.0067
17	0.0012	0.0066	0.0074
18	0.0096	0.0072	0.0054
19	0.0063	0.0035	0.0037
20	0.0015	0.0066	0.0074
21	0.0101	0.0052	0.0039
22	0.0028	0.0040	0.0051
23	0.0045	0.0060	0.0059
24	0.0073	0.0087	0.0040
25	0.0044	0.0063	0.0072
26	0.0117	0.0079	0.0057
27	0.0080	0.0059	0.0066
28	0.0044	0.0064	0.0082
29	0.0065	0.0082	0.0065
30	0.0070	0.0086	0.0060
31	0.0082	0.0061	0.0056
32	0.0051	0.0067	0.0053
33	0.0041	0.0057	0.0059
34	0.0022	0.0059	0.0050
35	0.0033	0.0047	0.0026
mean	0.0055	0.0066	0.0052
std. deviation	0.0035	0.0019	0.0013
cov	0.6468	0.2903	0.2449

Table B - 2 Maximum Drift for Model C-OBE

Motion #	Unscaled	ASCE	MPS
1	0.0114	0.0098	0.0043
2	0.0020	0.0056	0.0051
3	0.0061	0.0089	0.0048
4	0.0066	0.0084	0.0046
5	0.0094	0.0096	0.0044
6	0.0094	0.0096	0.0046
7	0.0102	0.0062	0.0053
8	0.0145	0.0104	0.0044
9	0.0106	0.0062	0.0048
10	0.0106	0.0068	0.0052
11	0.0083	0.0050	0.0045
12	0.0023	0.0057	0.0048
13	0.0039	0.0077	0.0043
14	0.0031	0.0074	0.0042
15	0.0114	0.0097	0.0045
16	0.0032	0.0052	0.0043
17	0.0008	0.0039	0.0040
18	0.0097	0.0076	0.0051
19	0.0086	0.0046	0.0053
20	0.0012	0.0049	0.0051
21	0.0120	0.0061	0.0048
22	0.0029	0.0042	0.0046
23	0.0044	0.0057	0.0049
24	0.0072	0.0086	0.0047
25	0.0034	0.0046	0.0051
26	0.0103	0.0074	0.0048
27	0.0065	0.0049	0.0042
28	0.0034	0.0051	0.0047
29	0.0058	0.0075	0.0048
30	0.0067	0.0086	0.0042
31	0.0081	0.0058	0.0046
32	0.0049	0.0066	0.0045
33	0.0039	0.0053	0.0048
34	0.0019	0.0053	0.0049
35	0.0047	0.0068	0.0053
mean	0.0054	0.0065	0.0047
std. deviation	0.0036	0.0018	0.0004
cov	0.6646	0.2814	0.0757

Table B - 3 Maximum Drift for Model B-MDE &MCE

	MDE		MCE	
Motion #	**ASCE**	**MPS**	**ASCE**	**MPS**
1	0.0168	0.0141	0.0290	0.0188
2	0.0127	0.0114	0.0164	0.0162
3	0.0129	0.0128	0.0158	0.0173
4	0.0119	0.0089	0.0230	0.0226
5	0.0235	0.0107	0.0383	0.0195
6	0.0170	0.0126	0.0212	0.0210
7	0.0120	0.0088	0.0162	0.0161
8	0.0175	0.0143	0.0206	0.0179
9	0.0115	0.0127	0.0158	0.0265
10	0.0108	0.0112	0.0142	0.0278
11	0.0111	0.0120	0.0140	0.0180
12	0.0113	0.0090	0.0230	0.0163
13	0.0121	0.0124	0.0159	0.0163
14	0.0117	0.0114	0.0228	0.0174
15	0.0233	0.0180	0.0291	0.0279
16	0.0161	0.0185	0.0215	0.0214
17	0.0119	0.0117	0.0185	0.0193
18	0.0214	0.0105	0.0383	0.0222
19	0.0081	0.0093	0.0134	0.0197
20	0.0149	0.0198	0.0270	0.0282
21	0.0116	0.0127	0.0159	0.0177
22	0.0094	0.0110	0.0107	0.0248
23	0.0148	0.0125	0.0189	0.0213
24	0.0216	0.0116	0.0320	0.0264
25	0.0172	0.0182	0.0198	0.0202
26	0.0136	0.0118	0.0232	0.0180
27	0.0125	0.0148	0.0293	0.0234
28	0.0146	0.0169	0.0214	0.0204
29	0.0152	0.0136	0.0298	0.0222
30	0.0166	0.0172	0.0182	0.0221
31	0.0099	0.0099	0.0183	0.0157
32	0.0143	0.0130	0.0189	0.0188
33	0.0115	0.0114	0.0132	0.0165
34	0.0103	0.0090	0.0149	0.0158
35	0.0121	0.0136	0.0171	0.0172
mean	0.0136	0.0125	0.0200	0.0200
std. deviation	0.0038	0.0029	0.0069	0.0038
cov	0.2816	0.2343	0.3423	0.1879

Table B - 4 Maximum Drift for Model C-MDE &MCE

	MDE		MCE	
Motion #	**ASCE**	**MPS**	**ASCE**	**MPS**
1	0.0191	0.0103	0.0336	0.0176
2	0.0119	0.0099	0.0162	0.0145
3	0.0164	0.0109	0.0195	0.0198
4	0.0146	0.0111	0.0223	0.0183
5	0.0219	0.0102	0.0360	0.0158
6	0.0177	0.0101	0.0261	0.0168
7	0.0156	0.0113	0.0233	0.0213
8	0.0178	0.0138	0.0281	0.0167
9	0.0118	0.0131	0.0140	0.0163
10	0.0116	0.0111	0.0166	0.0213
11	0.0120	0.0102	0.0170	0.0216
12	0.0122	0.0113	0.0235	0.0172
13	0.0125	0.0109	0.0177	0.0169
14	0.0170	0.0106	0.0236	0.0196
15	0.0164	0.0110	0.0244	0.0175
16	0.0126	0.0092	0.0214	0.0153
17	0.0089	0.0101	0.0180	0.0204
18	0.0207	0.0105	0.0337	0.0163
19	0.0120	0.0125	0.0198	0.0217
20	0.0105	0.0112	0.0170	0.0191
21	0.0132	0.0138	0.0167	0.0218
22	0.0099	0.0090	0.0151	0.0151
23	0.0144	0.0104	0.0224	0.0250
24	0.0172	0.0122	0.0252	0.0187
25	0.0097	0.0097	0.0156	0.0141
26	0.0143	0.0104	0.0252	0.0162
27	0.0119	0.0079	0.0200	0.0131
28	0.0102	0.0098	0.0187	0.0146
29	0.0142	0.0126	0.0239	0.0145
30	0.0117	0.0108	0.0173	0.0192
31	0.0133	0.0088	0.0213	0.0196
32	0.0150	0.0098	0.0185	0.0188
33	0.0130	0.0104	0.0220	0.0167
34	0.0131	0.0106	0.0192	0.0170
35	0.0130	0.0122	0.0192	0.0197
mean	0.0136	0.0107	0.0209	0.0178
std. deviation	0.0031	0.0013	0.0053	0.0027
cov	0.2279	0.1229	0.2528	0.1516

Table B - 5 Model B - OBE - Comparison of Motion Sets

		Unscaled Motion Sets				
		set1	**set2**	**set3**	**set4**	**set5**
	mean	0.0069	0.0041	0.0068	0.0049	0.0051
accuracy	**mean/benchmark**	1.2684	0.7561	1.2463	0.8962	0.9335
	std. deviation	0.0039	0.0037	0.0043	0.0033	0.0017
efficiency	**cov**	0.5604	0.8923	0.6339	0.6831	0.3287

	dispersion of means of sets	
	mean	0.0055
	std. deviation	0.0012
consistency	**cov**	0.2266

		MODEL B - OBE				
		ASCE Scaled Motion Sets				
		set1	**set2**	**set3**	**set4**	**set5**
	mean	0.0085	0.0061	0.0074	0.0060	0.0056
accuracy	**mean/benchmark**	1.5571	1.1255	1.3487	1.0990	1.0287
	std. deviation	0.0020	0.0010	0.0020	0.0017	0.0015
efficiency	**cov**	0.2364	0.1710	0.2772	0.2772	0.2603

	dispersion of means of sets	
	mean	0.0066
	std. deviation	0.0012
consistency	**cov**	0.1789

		MODEL B - OBE				
		MPS Scaled Motion Sets				
		set1	**set2**	**set3**	**set4**	**set5**
	mean	0.0053	0.0050	0.0053	0.0053	0.0053
accuracy	**mean/benchmark**	0.9751	0.9132	0.9725	0.9689	0.9733
	std. deviation	0.0007	0.0014	0.0015	0.0009	0.0019
efficiency	**cov**	0.1355	0.2873	0.2810	0.1737	0.3546

	dispersion of means of sets	
	mean	0.0052
	std. deviation	0.0001
consistency	**cov**	0.0277

Table B - 6 Model C - OBE - Comparison of Motion Sets

		Unscaled Motion Sets				
		set1	**set2**	**set3**	**set4**	**set5**
	mean	0.0067	0.0043	0.0065	0.0049	0.0051
accuracy	**mean/benchmark**	1.2326	0.7953	1.1989	0.8998	0.9457
	std. deviation	0.0035	0.0038	0.0048	0.0035	0.0018
efficiency	**cov**	0.5275	0.8922	0.7379	0.7242	0.3451

	dispersion of means of sets	
	mean	0.0054
	std. deviation	0.0010
consistency	**cov**	0.1920

		MODEL C - OBE				
		ASCE Scaled Motion Sets				
		set1	**set2**	**set3**	**set4**	**set5**
	mean	0.0082	0.0061	0.0068	0.0061	0.0056
accuracy	**mean/benchmark**	1.5096	1.1294	1.2613	1.1205	1.0402
	std. deviation	0.0016	0.0016	0.0024	0.0015	0.0011
efficiency	**cov**	0.1946	0.2610	0.3475	0.2481	0.1906

	dispersion of means of sets	
	mean	0.0065
	std. deviation	0.0010
consistency	**cov**	0.1533

		MODEL C - OBE				
		MPS Scaled Motion Sets				
		set1	**set2**	**set3**	**set4**	**set5**
	mean	0.0046	0.0047	0.0047	0.0046	0.0048
accuracy	**mean/benchmark**	0.8510	0.8654	0.8767	0.8455	0.8967
	std. deviation	0.0003	0.0005	0.0003	0.0003	0.0004
efficiency	**cov**	0.0688	0.1071	0.0597	0.0584	0.0799

	dispersion of means of sets	
	median	0.0047
	std. deviation	0.0001
consistency	**cov**	0.0238

Table B - 7 Model B - MDE - Comparison of Motion Sets

		MODEL B - MDE				
		ASCE Scaled Motion Sets				
		set1	**set2**	**set3**	**set4**	**set5**
	mean	0.0144	0.0129	0.0159	0.0128	0.0125
accuracy	**mean/benchmark**	1.1221	1.0058	1.2388	0.9996	0.9695
	std. deviation	0.0045	0.0036	0.0049	0.0028	0.0025
efficiency	**cov**	0.3137	0.2804	0.3075	0.2191	0.1979

	mean	0.0136
	std. deviation	0.0014
consistency	**cov**	0.1056

		MODEL B - MDE				
		MPS Scaled Motion Sets				
		set1	**set2**	**set3**	**set4**	**set5**
	mean	0.0117	0.0106	0.0145	0.0130	0.0129
accuracy	**mean/benchmark**	0.9122	0.8255	1.1311	1.0097	1.0081
	std. deviation	0.0017	0.0013	0.0038	0.0034	0.0024
efficiency	**cov**	0.1440	0.1266	0.2602	0.2605	0.1882

	mean	0.0125
	std. deviation	0.0015
consistency	**cov**	0.1184

Table B - 8 Model C - MDE - Comparison of Motion Sets

		MODEL C - MDE				
		ASCE Scaled Motion Sets				
		set1	set2	set3	set4	set5
	mean	0.0155	0.0139	0.0137	0.0125	0.0126
accuracy	mean/benchmark	1.3020	1.1710	1.1495	1.0529	1.0595
	std. deviation	0.0040	0.0039	0.0032	0.0017	0.0014
efficiency	cov	0.2552	0.2774	0.2348	0.1362	0.1145

	dispersion of means of sets	
	median	0.0136
	std. deviation	0.0012
consistency	cov	0.0887

		MODEL C - MDE				
		MPS Scaled Motion Sets				
		set1	set2	set3	set4	set5
	median	0.0107	0.0105	0.0114	0.0104	0.0107
accuracy	mean/benchmark	0.8962	0.8838	0.9547	0.8705	0.8999
	std. deviation	0.0005	0.0005	0.0019	0.0014	0.0017
efficiency	cov	0.0460	0.0498	0.1683	0.1327	0.1598

	dispersion of means of sets	
	mean	0.0107
	std. deviation	0.0004
consistency	cov	0.0357

Table B - 9 Model B - MCE - Comparison of Motion Sets

		MODEL B - MCE					
		ASCE Scaled Motion Sets					
		set1	set2	set3	set4	set5	set6
	mean	0.0212	0.0202	0.0225	0.0171	0.0195	0.0178
accuracy	mean/benchmark	1.0203	0.9723	1.0834	0.8238	0.9373	0.8531
	std. deviation	0.0087	0.0082	0.0061	0.0042	0.0069	0.0043
efficiency	cov	0.4083	0.4064	0.2696	0.2460	0.3519	0.2437

	dispersion of means of sets	
	mean	0.0196
	std. deviation	0.0021
consistency	cov	0.1045

		MODEL B - MCE					
		MPS Scaled Motion Sets					
		set1	set2	set3	set4	set5	set6
	mean	0.0193	0.0187	0.0214	0.0208	0.0199	0.0201
accuracy	mean/benchmark	0.9251	0.8974	1.0303	0.9977	0.9580	0.9666
	std. deviation	0.0040	0.0027	0.0053	0.0038	0.0025	0.0046
efficiency	cov	0.2091	0.1423	0.2487	0.1837	0.1270	0.2312

	dispersion of means of sets	
	mean	0.0200
	std. deviation	0.0010
consistency	cov	0.0499

Table B - 10 Model C - MCE - Comparison of Motion Sets

		MODEL C - MCE					
		ASCE Scaled Motion Sets					
		set1	set2	set3	set4	set5	set6
	mean	0.0238	0.0214	0.0207	0.0184	0.0208	0.0205
accuracy	mean/benchmark	1.2168	1.0949	1.0605	0.9411	1.0649	1.0511
	std. deviation	0.0076	0.0060	0.0049	0.0038	0.0019	0.0053
efficiency	cov	0.3219	0.2812	0.2354	0.2072	0.0917	0.2586

	dispersion of means of sets	
	mean	0.0209
	std. deviation	0.0017
consistency	cov	0.0829

		MODEL C - MCE					
		MPS Scaled Motion Sets					
		set1	set2	set3	set4	set5	set6
	mean	0.0178	0.0187	0.0181	0.0168	0.0175	0.0199
accuracy	mean/benchmark	0.9132	0.9578	0.9266	0.8596	0.8944	1.0193
	std. deviation	0.0019	0.0026	0.0024	0.0016	0.0044	0.00259
efficiency	cov	0.1092	0.1416	0.1345	0.0957	0.2515	0.13001

	dispersion of means of sets	
	mean	0.0181
	std. deviation	0.0011
consistency	cov	0.0596

APPENDIX C

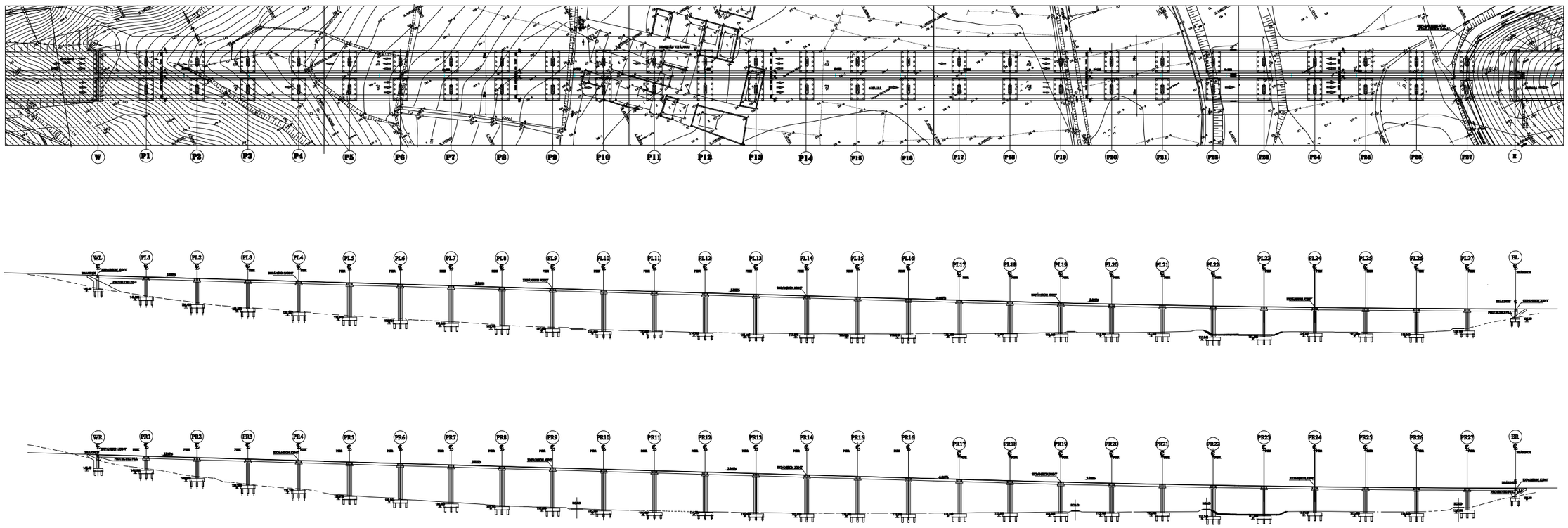

Figure C -1 Plan and Elevation View of Demirtas Viaduct